Male-specific reproductive failure caused by X-chromosomal substitution between two mouse subspecies

by Ayako Oka

Doctor of Philosophy

Department of Genetics

School of Life Science

The Graduate University for Advanced Studies

2001

CONTENTS

CHAPTER I Abstract

Consomic strains are defined as inbred strains, in which a certain chromosome of a strain is replaced as a whole by the same chromosome of another strain, leaving the rest of the former strain's chromosomes intact. I have set out to construct of a consomic mouse strain, replacing X-chromosome of a standard laboratory strain, C57BL/6J, by its homologue of a strain MSM. The gene pool of the most standard laboratory strains including C57BL/6J is known to have originated from a subspecies of west European wild mice, *Mus musculus domesticus*, while MSM was established from another subspecies of Japanese wild mice, *Mus musculus molossinus*. During generating the X-chromosomal consomic strain, B6.MSM-ChrX, I observed reduced fertility of the males that carry the MSM-derived X chromosome after the first backcross generation. It suggests the presence of epistatic interaction of an X-linked gene(s) and an autosomal and/or a Y-linked gene(s), which controls fecundity of male mice. The observed infertility is attributable to disruption of the interaction between the MSM allele(s) of the X-linked gene(s) and the C57BL/6J allele(s) of the autosomal and/or Y-linked gene(s).

In order to understand the genetic basis of the incompatibility of MSM and C57BL/6J alleles, I analyzed the phenotype of males that carry MSM-derived X chromosome in the background of C57BL/6J strain from the aspect of reproductive biology. To construct the consomic strain B6.MSM-ChrX, (C57BL/6J × MSM)F1 females were backcrossed to C57BL/6J males beyond 10 generations. At each

backcross generation, females carrying non-recombinant X chromosome of MSM were selected and mated with C57BL/6J males for the next generation. Hereafter, I refer to the males with non-recombinant MSM-derived X chromosome after the first backcross generation as X-MSM/Y, and to the males with non-recombinant C57BL/6J-derived X chromosome in the same litter as X-B6/Y. The males of the F1 hybrid were fertile, but the X-MSM/Y males of the first backcross generation (BCN2) exhibited slightly reduced fertility. The reduction in fecundity became clearer with the progression of the backcross generations. The X-MSM/Y males of the BCN9 generation no longer produced any progeny. At the same generation, the X-B6/Y males revealed full fecundity. Further analysis indicated that the spermatozoa of X-MSM/Y fail to fertilize eggs, or first cleavage of the fertilized eggs with the X-MSM/Y spermatozoa was blocked.

I observed that the weight of the testis of the X-MSM/Y males were 36% smaller than those of the control X-B6/Y males. Histological examination n revealed that the testis of X-MSM/Y males undergoes spermatogenesis, but has a spectrum of degeneration in the seminiferous tubules and interstitial space, with variation among the individuals.

Spermatozoa of C57BL/6J and MSM males have well-balanced, hook-shaped heads. In contrast, the X-MSM/Y males showed malformation of the sperm heads. Spermatozoa of the F1 hybrid of C57BL/6J and MSM strains retained normal morphology, but those of the first backcross generation (BCN2) exhibited slightly short and less curved distal part of the head. The malformation became much severer as the

backcross generations progressed. Eventually, the shape of sperm head became small and round. In addition to the morphological anomaly, I found that the motility was significantly lower in the X-MSM/Y spermatozoa than in the X-B6/Y spermatozoa.

In order to map the gene(s) responsible for the reduced fecundity of the X-MSM/Y males, I carried out quantitative trait loci (QTL) analysis with respect to the two traits, reduced testis weight and abnormal morphology of spermatozoa, because these two phenotypes seemed to be responsible for the reduction of the fecundity. The analysis successfully detected distinct QTLs for each phenotype on X chromosome. One of them, responsible for the reduced testis weight, was mapped to the interval between *DXMit97* and *DXMit249* in the distal region of X-chromosome. The other QTLs affecting spermatozoal morphology was mapped to three loci on X chromosome. The high likelihood ratios were located in the interval between *DXMit50* and *DXMit147* in the central region.

In the distal region of X-chromosome, there are several candidate genes, which are expressed in testis and may be responsible for the sterility. In the most distal region, furthermore, pseudoautosomal region is located, where X-Y pairing occurs. The structural incompatibility of MSM-derived X chromosome with C57BL/6J-derived Y chromosome may disturb association of X-Y chromosomes, and may result in disruption of normal spermatogenesis. In the central region of X chromosome, several candidate genes, which are expressed in the testis and are likely responsible for the abnormal spermatozoal morphology, have been mapped. One of them, a gene *Halap-X* encoding haploid-specific alanin-rich acidic protein is located on

Chromosome-X, which is expressed in the nucleoplasm of spermatids during the late stage of spermatogenesis, indicating the role in chromatin remodeling. Chromatin remodeling is a sequential exchange of chromatin proteins from histones to protaminees, which eventually leads to chromatin condensation. Mutant mice bearing abnormal chromatin remodeling are known to produce morphologically abnormal and immotile spermatozoa. I found a nucleotide sequence polymorphism between C57BL/6J and MSM in *Halap-X*. MSM has a coding sequence of 177 bp longer, than that of C57BL/6J. Thus, *Halap-X* is a good candidate for the QTL responsible for the abnormal spermatozoal morphology.

In conclusion, this study revealed that mouse X-chromosome has crucial genes involved in spermatogenesis through epistatic interaction with other genes in autosome(s) and/or Y-chromosome. It is most likely that the reproductive defects in males of the X-MSM/Y and the consomic strain B6.MSM-ChrX are due to disruption of the interaction by incompatibility of the MSM allele(s) of the X-linked gene(s) and the C57BL/6J allele(s) of the second gene(s) in autosome(s) and/or Y-chromosome. This disruption causes the reproductive isolation between two subspecies, *Mus musculus domesticus* and *Mus musculus molossinus*. (?)

CHAPTER II General introduction

During process of speciation, hybrids between two diverging populations of organisms show different extent of reproductive failure, which is referred to as "reproductive isolation". Reduction of fecundity of the hybrids prevents gene flow across the differentiating populations, and it may accelerate the speciation process. Eventually, it might contribute to evolution. Study of reproductive isolation is essential for understanding the process of speciation and evolution. It is also useful for understanding the genetic pathways underlying the reproduction system s.

Post-mating isolation is defined as a reproduction isolation, in which normal mating behavior is observed between the two populations. It can be classified into two categories. The first one is observed in F1 hybrids of the two populations. If the F1 hybrids show sterility, it is referred to as "hybrid sterility". The hybrid sterility follows Haldane's rule: if only one sex is sterile, it is always the heterogametic sex (Haldane et al., 1922). In mammals, it is the male. In mice, the reproductive isolation has been investigated in inter-specific or inter-subspecific crosses. However, its genetic basis and underlying molecular mechanism have been poorly understood. The hybrid sterility is assumed to be under the control of several different genes, designated as "hybrid sterility genes". The first detected hybrid sterility gene in mammals is *Hst1*, which is responsible for the sterility of inter-subspecific hybrids between a certain wild mouse of east European subspecies *Mus musculus musculus* and a standard laboratory strain, C57BL/10 (Forejt and Ivanyi, 1975). When the wild mouse was crossed with C57BL/10,

the F1 males become sterile with early spermatogenic disruption. On the contrary, when the same wild mouse was crossed with another laboratory strain C3H/Di, the resultant F1 males showed normal fecundity. The difference between C57BL/10 and C3H/Di with respect to the fertility is due to the allelic difference of *Hst1*. The C3H/Di allele, $Hst1^f$, is compatible with the allele of the wild mouse, $Hst1^w$, while the C57BL/10 allele, $Hst1^s$, is incompatible with $Hst1^w$. The heterozygous ($Hst1^s$ / $Hst1^w$) males become sterile. The *Hst1* locus was mapped to the *t*-complex region in chromosome 17 (Forejt and Ivanyi, 1975; Forejt et al., 1991; Trachtulec et al., 1997). Positional cloning of *Hst1* is now underway (Trachtulec et al., 1997). When the (C57BL/10 × the wild mouse)F1 females were backcrossed to C57BL/10 males, the males of the backcross progeny showed sterility with non-Mendelian segregation ratio; only less than 20 % of the progeny were sterile. This suggests that not only *Hst1* controls the sterility of the hybrid males, but also several additional *Hst* genes are involved in the sterility.

Inter-specific cross between *Mus musculus* carrying the *t*-haplotype and *Mus spretus* causes sterility specifically in the males. The responsible genes, *Hst4* (Pilder et al., 1991), *Hst5*, *Hst6* (Pilder et al., 1993) and *Hst7* (Pilder et al., 1997a; 1997b), were mapped to the distinct loci in the *t*-complex region of chromosome 17. The hybrids do not show spermatogenic arrest, but reduced motility and abnormal morphology of their spermatozoa were observed.

The *Hst3* locus was mapped close to the pseudoautosomal region in X chromosome from inter-specific cross between certain *M. m. musculus*-derived laboratory strains and *M. spretus* (Guenet et al., 1990). This sterility may be caused by

dissociation of X-Y pairing during spermatogenic meiosis, which is likely resulted from the structural X-Y incompatibility at the pseudoautosomal region between the two species. Recently, another X-linked hybrid sterility gene was mapped to the central region from crosses between C57BL/6J and *M. spretus*. It was designated as inter-specific hybrid testis weight 1 (*Ihtw1*), because males of the F1 hybrids revealed small and degenerated testes (Elliott et al., 2001).

The second category of the post-mating reproductive isolation is "hybrid breakdown", in which F1 hybrid is viable and fully fertile but F2 or the later generations show lowered viability and sterility. Hybrid breakdown is observed when a certain chromosome or a part of chromosome is substituted between two different mouse strains. It might be caused by disruption of interaction of alleles of the different strains at different loci, instead of allelic incompatibility at the same locus. If hybrid breakdown is observed in such a case, at least one of the genes must be located in the substituted chromosome. When Y chromosome of wild mouse, *M. m. domesticus*, collected in Poschiavinus was introduced into the genetic background of C57BL/6J, the Y-chromosome substituted strain, B6.Y^{POS}, showed defect in the testis development with sex reversal, so called hermaphrodites (Eicher et al., 1982). It was thought to be due to incompatibility between sex determining region in Y chromosome (*Sry*) allele on the POS-Y chromosome and C57BL/6J allele at the autosomal and/or X-linked loci. It also suggested that the Sry and autosomal and/or X-chromosomal genes interact during testis development. The genes involved in the testis-determining autosomal trait loci (*tda*) have been mapped to autosomes (Eicher et al., 1996).

As mentioned above, many genes involved in reproductive isolation have been studied in inter-specific crosses, such as *M. musculus* × *M. spretus*. When we investigate reproductive isolation, there is a drawback in the use of inter-specific hybrids. Two species of genus *Mus* diverged since at least 3 million years ago, and they have accumulated large genetic diversity. Hence, many genes are involved in the reproductive failures in the inter-specific hybrids. This hampers genetic analysis to dissect a single gene concerned with the reproductive isolation. This is crucial particularly in analysis of genes that function in early stage of speciation. From this aspect, crosses between the laboratory strain C57BL/6J (*M. m. domesticus*) and Japanese wild mouse-derived MSM strain (*M. m. molossinus*) are thought to be the ideal experimental system. They diverged from a common ancestral species *M. musculus* approximately 1 million years ago. The F1 males are fully fertile, and the reproductive isolation between the two populations has not been completed. However, introduction of certain genes across these strains causes sterility, which may reflect the initiation event of the reproductive isolation in speciation process.

Previously, Takagi et al. introduced X chromosome of MSM strain onto the C57BL/6J genetic background using reproductive C57BL/6J-X0 females that carry hemizygous X chromosome. Since no homologous recombinations occur through the whole X chromosome in the XO females, it was possible to introduce the MSM-derived X-chromosome as a whole into C57BL/6J strain (Takagi et al., 1994). The resultant strain represented the sterility with abnormal spermatozoa. This implies that the incompatibility between X-lined gene(s) and autosomal and/or Y-linked

gene(s) cause reproductive isolation.

Since several years ago, Mammalian Genetics Laboratory of National Institute of Genetics (NIG) has set out to construct a series of consomic strains, in each of which a certain chromosome of a strain is replaced by its homologue of another strain, leaving the rest of the former strain's chromosomes intact. As mouse has 19 autosomes and two sex chromosomes, X and Y, totally 21 independent consomic strains have been generated. In this project, C57BL/6J is used as the chromosome recipient strain and MSM as the donor strain. This full set of inter-subspecific consomic strains covers the whole genome of the donor strain MSM.

To obtain an independent line of evidence for the hybrid breakdown, and to clarify the genetic basis of reproductive isolation that involves X-chromosome, I analyzed the phenotypes of the reproductive system of mice that carry non-recombinant X-chromosome of MSM on the C57BL/6J genetic background. To do this, females heterozygous for the non-recombinant MSM-derived X chromosome and the C57BL/6J-derived X chromosome (X-MSM/X-B6) were selected at different backcross generations to establish the X chromosomal consomic strain, and they were backcrossed to the C57BL/6J males. In the present study, it was discovered that F1 hybrid males retained their fertility, but males with non-recombinant X chromosome of the MSM strain, X-MSM/Y, started to show reduction of the fecundity after the first backcross generation (BCN2). The fecundity further decreased as the backcross generations proceeded. This indicated that the male sterility was caused by disruption of the interaction of MSM-derived X chromosome and autosomal and/or Y-linked

genes of the C57BL/6J background.

Subsequently, I conducted to map the X-linked gene(s) responsible for the reproductive isolation. For this purpose, I carried out Quantitative Trait Loci (QTL) analysis for the phenotypes of the X-MSM/Y males, using the progeny generated from the backcross of heterozygous females, X-MSM/X-B6, to C57BL/6J males. From this analysis, I successfully found distinct QTLs on the X chromosome, one in the distal region and another in the central region, which are responsible for the reduction of testis weight and abnormal morphology of the sperm head, respectively. These X-linked genes may function in the male reproduction system particularly in spermatogenesis, in cooperation with interactive gene(s) on other chromosome(s).

Study of the genetic mechanism of the sterility using this experimental system should provide a new insight into the reproductive isolation and speciation process. Moreover, further genetic analysis of both X-linked gene(s) and the interactive genes on the other chromosomes would shed light on understanding of the genetic pathways of mammalian spermatogenesis.

CHAPTER III Phenotype characterization of males that carry MSM-derived X chromosome in the C57BL/6J background.

1. Introduction

On the way to the establishment of a series of inter-subspecific consomic strains, I observed reduced fertility only in the males that carry MSM-derived X chromosome, X-MSM/Y. It suggested incompatibility of the X chromosome of MSM strain with autosome(s) and/or Y chromosome of C57BL/6J strain.

In this Chapter, I made in-depth characterization of the reduced fecundity of X-MSM/Y males. First, I evaluated the fecundity of the X-MSM/Y males generated at different backcross generations, BCN2, BCN3, and BCN9, by caging the males with C57BL/6J females. The result showed that males of (C57BL/6J × MSM)F1 hybrids were fertile, but the males of the first backcross generation, BCN2, showed slightly reduced fecundity. The reduction was further augmented at the BCN3 generation, and the males at the BCN9 generation were revealed to be fully sterile.

In order to examine the cause of the sterility, I collected two-cell-stage embryos or unfertilized eggs from oviducts of superovulated females mated with X-MSM/Y males by flushing with medium two days after copulation. The result showed the absence of two-cell-stage embryos, which should be collected from the oviducts in regular mating with C57BL/6J males.

In the phenotype characterization of the X-MSM/Y males, it appeared that X-MSM/Y males had smaller testes size as compared with the X-B6/Y males in the

same littermate. Histological analysis of the testes revealed various degrees of degenerated spermatogenesis with variation among individuals. In addition, I observed shortened sperm heads. Transmission electron micrograph indicated that the sperms heads had abnormal figure of the nuclei and the acrosomes. The electron density of the nuclei, however, appeared normal and acrosome formation was intact. In addition to the morphological anomaly, significantly low motility was observed in the spermatozoa of the X-MSM/Y males by sperm quality analyzer.

2. Materials and methods

Mice:

C57BL/6J was purchased from the Jackson Laboratory (Bar Harbor, MA., USA), and has been maintained in the animal facility at the National Institute of Genetics (NIG, Mishima, Japan), or was purchased from CLEA Japan (Tokyo, Japan) where C57BL/6J from the Jackson Laboratory has been maintained. MSM strain was established at NIG and was derived from the Japanese wild mouse, *Mus musculus molossinus* (Moriwaki, 1994; Bonhomme and Guenet, 1996).

Consomic strain:

(C57BL/6J × MSM)F1 females were backcrossed to C57BL/6J males for 10 generations (Fig. 1A). Females with non-recombinant X chromosomes from the MSM strain were selected by genotyping at least 10 microsatellite markers at intervals of approximately 10 cM through the X chromosome (Fig. 1B), and were mated with C57BL/6J males at each backcross generation. The mice generated by this mating eventually had non-recombinant X chromosome from MSM in the genetic background of C57BL/6J strain.

Microsatellite markers:

Following microsatellite markers, which show polymorphism between C57BL/6J and MSM strains, were used in this study: *DXMit89, DXMit72, DXMit50, DXMit109,*

*DXMit147, DXMit95, DXMit97, DXMit217, DXMit249*and *DXMit160*, which are located at 3.0, 4.8, 14.1, 27.0, 33.5, 43.0, 49.0, 63.0, 70.5 and 73.3 cM from the centromere, respectively. The PCR primers for the above markers were purchased from Research Genetics (Huntsville, AL., USA) or were ordered for RIKAKEN (Nagoya, Japan) and Sawaday technology (Tokyo, Japan) to synthesize them, using information from the database of Whitehead Institute for Biomedical Research (Cambridge, MA., USA, http://www-genome.wi.mit.edu/). Information for SSLP of the microsatellite markers was obtained from the Mouse Microsatellite Data Base of Japan (MMDBJ) (NIG, Mishima, Japan, http://www.shigen nig. ac.jp/mouse/mmdbj/mouse.html).

PCR genotyping:

Genomic DNA for genotyping was prepared from ear or liver. The PCR-amplified DNAs with the primer sets were separated on electrophoresis gel with 4 % agarose (3 : 1 ratio of Nusieve : Seakem agarose) (FMC Bioproducts, Me., USA) in 1× TAE buffer. The DNA bands visualized by ethidium staining were analyzed.

Analysis of fertility in natural mating:

Individual of 3-4 month aged males was caged with three 2-3 month aged C57BL/6J females for 10 days, and then they were separated. These females were dissected after the additional 10 days and the number of embryos was counted. Approximately 10 days before the test mating, a male was pre-mated with a C57BL/6J female for replacement of old spermatozoa in the epididymis and stimulation of spermatogenesis.

Analysis of fertilization in vivo:

For analysis of fertilization *in vivo*, 2 months aged C57BL/6J female was superovulated by i.p. injection of 5 units PMSG (TEIKOKU HORMONE Mfg., Tokyo, Japan), and followed by 5 units hCG (TEIKOKU HORMONE Mfg., Tokyo, Japan) 46-48 hrs after the PMSG injection, and then the female was mated with a 3-4 months aged male. Females with copulatory plugs on the following morning were dissected to collect eggs/embryos from the oviducts 2 days after the copulation. Eggs/embryos were flushed with WT medium (Whittingham et al., 1972) from the oviducts. They were divided into three types: unfertilized eggs, two-cell-stage embryos and abnormal eggs.

Histology of testes:

At 3-4 months of age, males were dissected and pairs of testes were weighted. Testes and epididymis were placed in fresh Bouin's fixative at room temperature. Excess fixative was removed with 70% ethanol. Tissues were then dehydrated and embedded in paraffin for microtome sections. The sections (6 μm) were stained with hematoxylin and eosin.

Analysis of spermatozoal morphology:

For morphological analysis, spermatozoa were obtained from the cauda epididymis and were observed under phase contrast microscope. For transmission electron microscopy

(TEM) observation, testes were fixed by perfusion *via* the left ventricle with 2.5 % glutaraldehyde in 0.1 M cacodylate buffer. The removed testes were further immersed for 2 hrs in the same fixative, washed thoroughly, and then cut into small pieces. The small pieces were fixed with 2 % osmium tetroxide, routinely dehydrated and embedded in Epon 812 (Toshimori and Oura, 1993). Ultrathin sections were made with a diamond knife on an ultratome (LKB model 2088, LKB-Producter AB, Bromma, Sweden), and double-stained with uranium acetate and lead citrate in an autostainer (LKB model 2168). Observation was done under transmission electron microscope at 75 kV accelerating voltage (H7100 type, HITACHI, Japan).

Sperm motility assay:

Spermatozoa were collected from the cauda epididymides of males. The distal portion of the epididymis was cut using a blade, and a dense sperm mass was squeezed out. For the capacitation of spermatozoa, the squeezed sperm mass was dispersed into TYH medium (Toyoda et al., 1971) under paraffin oil and were incubated at 37° in 5 % CO2. After 1, 2, 3 and 4 hrs of the incubation, spermatozoa were examined for calculation of the sperm motility index (SMI) by Sperm Quality Analyzer-SQAII C (Unite Medical System Inc., Ca., USA). Number of spermatozoa was counted with hemocytometer, and each SMI value was standardized with the number of spermatozoa, 10^7/ml.

Radioimmunoassays of hormone:

Serum samples were sent to SRL, Ltd., Tokyo, Japan for assay of testosterone. The

assay was done using Coat-A-Count kits (Diagnostic Products Corp., Ca., USA), according to the manufacturer's instructions.

3. Results

3.1 Reduced fecundity in natural mating

As a control experiment, nine C57BL/6J males were respectively caged with three C57BL/6J females for 10 days. As a result, 6 out of 9 males appeared to be reproductive, and they made 13 out of 30 females pregnant with the average litter size of 7.9. When (C57BL/6J × MSM)F1 males were tested, 9 out of 10 males were reproductive and they made 17 out of 29 females pregnant with the average litter size of 7.4. The fecundity of these males was not significantly different from that of the control C57BL/6J males (Table 1). At the first backcross generation, BCN2, 9 out of 10 X-MSM/Y males were reproductive, but the average litter size decreased to 5.0. The X-MSM/Y males of the next generation, BCN3, exhibited marked reduction in fertility. Only 2 out of 10 males were reproductive, moreover the litter size of the offspring and the frequency of pregnant females decreased significantly. At the BCN9 generation, all males with MSM-derived X chromosome, X-MSM/Y, were fully sterile. On the contrary, males with X-B6/Y, at the same BCN9 generation showed full fertility. The frequency of pregnant females from the above cross was comparable to that obtained in the cross with C57BL/6J males, and the litter size was normal. The females heterozygous for X chromosomes, X-MSM/X-B6, were always fertile and showed no significant reduction in the litter size during all the backcross generations when they were crossed with C57BL/6J males.

3.2 Defects in fertilization in cross with X-MSM/Y males

When each of eighteen X-MSM/Y males, which were generated from the BCN7 –8 backcross generations, was caged with a superovulated C57BL/6J female for one day, eight males produced copulation plugs. This rate was similar to that observed in crosses with the control X-B6/Y males at the same generations, in which 9 out of 17 males produced copulation plugs. Two days after the copulation, eggs/embryos were collected from oviducts of the females with the copulation plugs. Total number of collected eggs/embryos was not significantly different between the crosses with X-B6/Y and with X-MSM/Y males. From the females mated with X-B6/Y males, 78.1 % of the flushed eggs/embryos were two-cell stage embryos, and most of the embryos successfully developed to blastocysts. On the contrary, two-cell stage embryos were never found in the females mated with the X-MSM/Y males (Table 2).

3.3 Reduced testis weight

The X-MSM/Y males at the BCN5 - 7 generations had body weight similar to that of the X-B6/Y males at the same generations (Table 3). However, the average testis weight of the X-MSM/Y males showed a 36.1 % reduction compared with that of the X-B6/Y males (Table 3). Cryptorchidism did not occur in the X-MSM/Y males and reproductive organs other than the testis appeared normal.

3.4 Abnormal testicular histology

At different stages of spermatogenesis, the germ cells reside in distinct location within seminiferous tubules, and nucleus of the germ cell differs both in morphology and size. Spermatogonia located along the basal lamina are dividing mitotically, and they differentiate into spermatocytes that form an inner layer of cells. They further undergo meiotic divisions twice and develop into spermatids, which subsequently differentiate into spermatozoa before being released into the lumen (Fig. 2A and 2E). Histological examination of the testis of the X-MSM/Y males at BCN8 revealed that the testis had various degree of degeneration in the seminiferous tubules and interstitial space. Similar degeneration was sometimes observed even in the X-B6/Y testes, but in most of the cases the degeneration was much milder than in the X-MSM/Y males (Fig. 2B and 2F). The X-MSM/Y males exhibited a spectrum of degeneration in seminiferous tubules with variation among individuals: some tubules showed severe disruptions in spermatogenesis (Fig. 2D and 2H), and others showed abnormal but ongoing spermatogenesis (Fig. 2C and 2G). Extremely degenerated seminiferous tubules had thin and irregular epithelia, developing spermatocytes and spermatids sloughing into the lumen, and a small number of spermatogonia and Sertoli cells retained along the basal lamina (Fig. 2H). Most of the sloughing germ cells did not show apoptotic cell death. Severely degenerated seminiferous tubules tended to locate in the middle of the testes.

Hyperplasia and hypertrophy of Leydig cell were observed in the interstitial space adjacent to the severely degenerated tubules (Fig.2D). Even in the peripheral seminiferous tubules, where spermatogenesis was taking place, decreased number of

germ cells, increased apoptotic germ cells, disrupted array and fragile adhesion within the germinal layers were observed (Fig. 2G). The cauda epididymal lumina of the X-B6/Y males were filled with matured spermatozoa (Fig. 2I), while that of the X-MSM/Y males contained both matured spermatozoa and many abnormally developing germ cells (Fig. 2J).

I measured testosterone level in serum, because Leydig cells produce testosterone and the high level of testosterone concentration in the serum of the X-MSM/Y males was expected due to the hyperplasia of Leydig cells. The average testosterone level of the X-MSM/Y males at theBCN6 generation, however, did not differ from that of C57BL/6J and the X-B6/Y males at the same generations: C57BL/6J, 1.80 ng/ml ± 2.48; X-B6/Y, 1.02 ng/ml ± 1.67; X-MSM/Y, 1.30 ng/ml ± 2.08 (n=5).

3.5 Light micrograph of abnormal morphology of the X-MSM/Y spermatozoa

Most epididymal spermatozoa from C57BL/6J males had well-balanced, hook-shaped heads (Fig. 3A). In contrast, the X-MSM/Y males at the BCN2 generation exhibited slightly short distal region of the sperm heads (Fig. 3C). This morphological malformation in sperm heads was augmented at the BCN3 generation, and it was observed at high frequencies (> 90 %) after the BCN3 generation. The distal part of the spermatozoa became short and less curved in the X-MSM/Y males (Fig. 3D). In the extreme case, the distal part of the sperm head was lost, and the sperm head became small and round. Reproductive (C57BL/6J × MSM)F1 males did not show abnormal

morphology in the spermatozoa. Likewise, theX-B6/Y spermatozoa had the normal head shape through the progression of the backcross generations (Fig.3B). In addition to the anomaly in the sperm head, spermatozoa with abnormal midpiece attachment was frequently observed in the X-MSM/Y males, which occurred at unpredictable frequency in C57BL/6J and the X-B6/Y males as well.

3.6 Transmission electron micrograph of abnormal morphology of the X-MSM/Y spermatozoa

Observations with transmission electron microscope (TEM) revealed that epididymal spermatozoa of the X-B6/Y males had regular thin spindle-shaped sperm heads (Fig. 4A and 4C). On the contrary, the X-MSM/Y males exhibited abnormalities in their sperm head (Fig. 4B). Most of the sperm heads had irregular, enlarged, curved and hook-shaped or mashroom-shaped figures (Fig. 4E and 4F). Chromatin condensation seemed to occur, because the electron density of the sperm nuclei of the X-MSM/Y was as high as that of X-B6/Y males. Malformation of acrosome morphology, possibly resulted from abnormal nuclear shapes was observed, but acrosome appeared discontinuous between sperm cell membrane and acrosomal membrane (Fig. 4D).

3.7 Reduced sperm motility

In order to assess the motility of spermatozoa, spermatozoa were incubated in TYH medium under 5 % CO2, and the values of sperm motility index (SMI) of each male was calculated by Sperm Quality Analyzer-SQAII C at an interval of 1h. The value of

SMI reflects both the concentration of motile spermatozoa and the intensity of their motility (Bartoov et al., 1991). The SMI values of the X-B6/Y and the X-MSM/Y males showed typical temporal changes in the sperm motility (Fig. 5). The SMI values of the both strains reached a peak of the activity after 2 hrs and decreased gradually. The X-B6/Y males exhibited normal SMI value, whereas the mean SMI value of the X-MSM/Y males was significantly lower than that of the X-B6/Y males through the time course of the sperm incubation. Spermatozoa of the X-MSM/Y males appeared to be defective in both the two quantities of the SMI, the concentration of motile spermatozoa and the intensity of the motility.

4. Discussion

4.1 Declining fecundity in X-MSM/Y males during the successive backcrossing

Males of (C57BL/6J × MSM)F1 hybrids were fully fertile, whereas the X-MSM/Y males showed declining fecundity with the progression of backcrosses generations after the BCN2. On the contrary, the X-B6/Y males had remained their fertility through all the backcross generations. Thus, it is clear that the sterility of the X-MSM/Y males is caused by disruption of epistatic interaction between X-linked gene(s) and autosomal and/or Y-linked gene(s). The stepwise declining of the fecundity of the X-MSM/Y males through the BCN2-3 backcross generations indicated that not a single but multiple autosomal and/or Y-linked genes are involved in the epistatic interaction.

4.2 Reduced fertility and defects in testicular histology

Histological analysis of the testes of the X-MSM/Y revealed that the spermatogenesis occurs to some extent in these males, but I found various degree of degeneration of the formation of the seminiferous tubules and the interstitial space among the individuals. The number of the–spermatogenic cells including spermatozoa was reduced in the X-MSM/Y males as compared with that of the X-B6/Y males. The disruption of the spermatogenesis may be the reason for the reduction of the testis weight in the X-MSM/Y males, because the two phenotypes were well correlated among different individuals. However, it may not be directly responsible for the sterility, because most of the X-MSM/Y males could produce substantial amount of spermatozoa and the

X-B6/Y males also showed similar phenotype though the frequency was much lower.

In the severely degenerated testes, the interstitial space was expanded and was filled with proliferating Leydig cells. The hyperplasia of the Leydig cells tended to be localized in the interstitial spaces adjacent to the severely degenerated seminiferous tubules, which is commonly observed as a response to germ cell degeneration. Leydig cells are the primary source of testicular testosterone and have a critical endocrine function to regulate spermatogenesis. Therefore, the hyperplasia might be explained as the result of response of Leydig cells to the feedback regulation of the hypothalamus and pituitary gland by luteinizing hormone (LH), which is stimulated by disrupted spermatogenesis. If this is the case, levels of serum testosterone should be higher in the X-MSM/Y males. The result showed that the serum testosterone level was, however, normal, indicating that the hyperplasia is not caused by the feedback regulation.

It was previously reported that (C57BL/6 × *Mus spretus*)F1 males showed high frequency of dissociation of X-Y pairing in the pachytene stage, which resulted from the genetic divergence in the pseudoautosomal region between the two species. It leads to a developmental arrest at metaphase I, and subsequently spermatocyte degeneration (Matsuda et al., 1991). It is likely that the genetic divergence between C57BL/6J and MSM strains in the pseudoautosomal region causes dissociation of X-Y pairing and accounts for the partial spermatogenic breakdown in the X-MSM/Y males.

4.3 Reduced fecundity and anomaly in spermatozoa

Normal male mouse ejaculates approximately 5.8×10^7 spermatozoa into the

reproductive tract at one time. Some spermatozoa reach the ampulla of the oviduct within 5 minutes, but they are not competent for fertilization for about 1 hour until capacitation, a process of sperm maturation occurs. Before reaching the surface of eggs, spermatozoa penetrate the cumulus mass first, and then the zona pellucida. Spermatozoa release various hydrolytic enzymes from acrosome (a secretory vacuole-like structure in the sperm head) to digest the zona pellucida.

The X-MSM/Y produced vaginal copulation plugs at almost the same frequency as the X-B6/Y males did, indicating their ordinary sexual behavior. However, I found no two-cell stage embryo in the oviducts of the females mated with the X-MSM/Y males. There are two possible interpretations for this. Firstly, spermatozoa of the X-MSM/Y may not be able to reach eggs in the oviduct or they cannot fertilize eggs. Alternatively, fertilized eggs cannot undergo the first cleavage. In order to test the first possibility, I investigated the morphology of spermatozoa from the X-MSM/Y males. The number of spermatozoa squeezed from the cauda epididymis of X-MSM/Y was slightly smaller than that of X-B6/Y, but adequate for fertilization (X-MSM/Y, 7.9×10^6 and X-B6/Y, 12.6×10^6). The spermatozoa of the X-MSM/Y exhibited severe morphological abnormality in their heads. The malformation possibly impairs fertilization of the X-MSM/Y males at the following two steps: swimming up of sperms through the female reproductive tracts to reach eggs in the ampulla, and penetration of sperm into cumulus or zona pellucida of eggs. Normal hook-like shape of the sperm head helps fusion of sperms and eggs. Therefore, the loss of the normal morphology of the distal part of the sperm head in the X-MSM/Y males may impair

binding of the spermatozoa to the surface of eggs and penetration across the cumulus mass and zona pellucida. In addition, the spermatozoa of the X-MSM/Y males exhibited remarkably lower motility. It may reduce the rate of the X-MSM/Y spermatozoa to reach eggs through female reproductive tract.

Thus, all these data indicated that the X-MSM/Y spermatozoa have a defect in fertilization. At present, however, the second possibility that eggs fertilized with X-MSM/Y spermatozoa are unable to undergo the first cleavage remains to be tested. To clarify this, formation of the male pronucleus or the extrusion of second polar body should be examined.

4.4 Abnormal morphology in spermatozoa and abnormal condensation of sperm nuclei

During spermiogenesis, chromatin remodels through sequential exchanges of chromatin protein from histones to protamines, Prm1 and Prm2, *via* transitional proteins, TP1 and TP2, which finally causes chromatin condensation in sperm nuclei. Knockout mouse mutants for the genes encoding the above proteins showed morphological abnormality and immotile spermatozoa. Male chimeras with disrupted *Prm1* or *Prm2* gene (Cho et al., 2001) and null mutant mice for *TP1* (Yu et al., 2000) were reported to have such phenotypes. Knockout null mutant for Ca^{2+}/calmodulin-dependent protein kinase IV gene (*Camk4*), which possibly functions in the exchange of basic nuclear proteins during spermiogenesis, also showed similar phenotype (Wu et al., 2001). All these reports suggest a strong correlation between

chromatin remodeling and spermatozoal morphology and motility. Though transmission electron microscopic analysis in this study revealed that the X-MSM/Y spermatozoa undergo condensation of the sperm nuclei, it is not still clear whether the proper exchange of chromatin proteins occurs in these spermatozoa. It is also known that the chromatin proteins are translationally regulated and premature translation of protaminee 1 leads to precocious nuclear condensation and sterility (Lee et al., 1995). Future analysis of both transcriptional and translational regulation of these chromatin proteins would answer the question as to whether proper chromatin condensation takes place in sperm nuclei of the X-MSM/Y males.

CHAPTER IV Quantitative trait loci (QTL) analysis of X-chromosomal factor(s) responsible for the sterility of X-MSM/Y males

1. Introduction

The sterility of the X-MSM/Y males seems to be caused by a discoordination between X-linked factors of the MSM strain and autosomal and/or Y-linked factors of the C57BL/6J strain. The number of genes interactive with the X-chromosomal factors may not be many, because most of the X-MSM/Y males became completely sterile by the BCN3 generation, in which 12.5 % of the whole genome is of MSM origin.

In this chapter, I conducted mapping of the genetic determinants on the X-chromosome, which are responsible for the sterility of the X-MSM/Y males. In the mapping, I focused on two phenotypes, the reduced testis weight and the morphological anomaly of spermatozoa. Since these phenotypes are quantitative traits, I applied Quantitative Trait Loci (QTL) analysis for mapping of these phenotypes. The QTL analysis is a powerful tool for identifying genetic loci that determine quantitative traits, which are usually controlled by multiple genes. Recently, QTL analysis has been improved by use of the abundant information for polymorphic markers, represented by microsatellite markers, and by the development of sophisticated statistical methods of mapping algorisms (Basten et al. 1996; Manly and Olson, 1999). After the BCN5 backcross generation, most part of the genome of the X-MSM/Y mouse was replaced by C57BL/6J chromosomes except for the X-chromosome. The percentages of C57BL/6J-derived genome for the whole genome at each generation are: BCN5,

96.9 %; BCN6, 98.4 %; BCN7, 99.2 %. The genetic background of the X-MSM/Y males can be considered almost the same as that of C57BL/6J after BCN5 generation. For this reason, I carried out QTL analysis only for the X chromosome, based on the backcross progeny generated from the heterozygous X-MSM/X-B6 females. In the analysis, I pooled the progeny from the BCN5- 7 backcross generations, ignoring other chromosomal effects.

The QTL analysis required quantification of phenotypes to be analyzed. In this study, I analyzed the phenotypes that meet the following conditions; 1) it reflects the male fecundity, 2) it is easy to quantify, and 3) the quantification is objective. Thus, testis weight and spermatozoa morphology were chosen as the quantitative traits in the analysis. For the objective quantification of spermatozoal morphology, more than 100 epididymal spermatozoa were observed and classified into 6 levels regarding the severity of morphological anomaly, and finally the trait of the individual was quantified as a score.

As a result of the analysis, the QTLs controlling reduced testis weight and spermatozoal anomaly were mapped to the distal and the central region of X chromosome, respectively. In the central and distal regions, there are several candidate genes, which are expressed in testis and may be responsible for the sterility. In the distal region, moreover, sterility associated with X-Y dissociation at the pseudoautosomal region has been reported in hybrid males of C57BL/6J and *M. spretus* (Matsuda et al. 1982). In this Chapter, I discuss the genetic determinants for the phenotypes of the X-MSM/Y males and the candidates for the QTLs.

2. Materials and methods

Preparation and measurement of spermatozoa:

Spermatozoa from cauda epididymis were stained with 2 % trypan blue (E. Merck, Darmstadt, Germany) and Giemsa's stain solution (Nakalai Tesque, Kyoto, Japan) as described (Didion et al., 1989). Spermatozoa preparation was observed under light microscope.

QTL analysis:

Totally, 179 progeny were collected from the BCN5, BCN6 and BCN7 backcross generations, and they were examined for the following two traits: reduced testis weight and morphological anomaly of spermatozoa. Genotypes of the progeny were determined for twelve microsatellite markers indicated in Fig. 1B. I carried out composite interval mapping analysis (Zeng, 1994) with a program "QTL Cartographer" (Basten et al. 1996), which provides the likelihood ratio (LR) test statistic for testing and estimates of additive and dominance effect of a QTL. Because the traits of only males were analyzed, the dominance effect of a QTL could not be estimated. The hypotheses for testing are: H_0, no QTL effect at the tested position, namely, a (the additive effect of a putative QTL) = 0; H_1, there is a QTL effect at the tested position, namely, $a \neq 0$. I used Model 6 of Zmapqtl. This model uses the most important markers to control for the genetic background. The likelihood test statistics is: $-2 \ln (L_0/L_1)$, where L0 is the maximum likelihood under the null hypothesis H_0, and L_1 is the maximum likelihood under the

alternative hypothesis H_1. The LR test statistic = 2 × (ln10) × LOD (= 4.61 × LOD). The 5% critical value may be taken as $\chi^2_{0.05/12=0.0042}$(D.F. = 2) = 11.0.

Polymorphism analysis of Halap-X gene:

For examining polymorphisms in the nucleotide sequence of *Halap-X* between C57BL/6J and MSM strains, DNA fragments containing the full-length coding region of *Halap-X* were PCR-amplified by A8 primer pair (Forward: 5'-CCCGAGCTCTCGAGGTAGCA-3', Reverse: 5'-GTCGTGACTCTATCGGTAGA-3'), using the cDNA from the testes of each strain as templates. The fragments were cloned and sequenced completely for their coding regions.

3. Results

3.1 QTL analysis of X-chromosomal factor(s) responsible for the reduced testis weight

Totally, 179 male progeny of the BCN5-7 backcross generations was analyzed for detecting the QTLs responsible for the testis weight. The testis weights of the progeny showed normal distribution pattern ranging from 34.7 mg to 131.7 mg. The X-B6/Y males had the average testis weight of 94.4 mg, while the X-MSM/Y males 60.3 mg. The result is graphically summarized in Fig. 6. The LR test statistic scores have a single peak located at the distal region of X chromosome, between *DXMit97* and *DXMit249*. The scores within the interval between *DXMit109* and *DXMit249* exceed 5 % critical value. The maximum LR score of 129.1 lies on *DXMit217*, and the estimated additive effect was 15.5 mg. This QTL explains 90.9 % of the difference in the average testis weights between the X-B6/Y and X-MSM/Y males.

3.2 QTL analysis of X chromosomal factor(s) responsible for the abnormal morphology of spermatozoa

The male progeny of the BCN5-7 backcross generations showed a wide range of variation in the morphology of the spermatozoa. First, I classified the sperm head anomaly into the following 6 types with respect to the level of morphological anomaly. Fig. 7 illustrates their schematic morphology and the classification. Type 1 spermatozoa have a normal morphology as observed in the C57BL/6J and MSM males. Type 2 has a

slightly shortened distal region. Type 3 has an entirely narrowed sperm head in addition to the slightly shortened distal region like Type 2. Type 4 shows a severely shortened distal region and a squared postal region. Type 5 has lost the entire distal region and has a squared postal region. Type 6 is characterized by a small and round sperm head. Because an abnormal midpiece attachment occurred at unpredictable frequency not only in the X-MSM/Y males but also in the C57BL/6J and X-B6/Y males, this kind of spermatozoa was ignored in the present analysis. For the objective quantification, more than 100 spermatozoa from each male were classified into the above 6 types, and the percentage of each type was calculated. As shown in Fig.7, the majority (87.0 %) of spermatozoa from the X-B6/Y males were classified into type 1, while 71.0 % of spermatozoa from the X-MSM/Y males were classified into type 4. To quantify the morphological anomaly of spermatozoa for QTL analysis, I evaluated each male by scoring the degree of the anomaly. To do this, I gave points from 0 to 5 to these 6 types, respectively, and obtained net score of the individuals according to the following formula: net score of individual = {0 × (% of type 1)}+ {1 × (% of type 2)}+ {2 × (% of type 3)}+ {3 × (% of type 4)}+ {4 × (% of type 5)}+ {5 × (% of type 6)} In this formula, high score stands for severe anomaly and low score weak anomaly. For example, the average net score of the X-B6/Y and the X-MSM/Y males were calculated as 19.8 and 326.2, respectively. The male progeny of the BCN5-7 backcross generations showed a distribution of the score, ranging from the lowest 0 to the highest 394.1.

The result of the QTL analysis based on 179 male progeny is graphically summarized in Fig. 8. The LR test statistic scores show three peaks distributed through

the X chromosome. The highest peak is located in the interval between *DXMit50* and *DXMit147*, the secondary one is located in the interval between *DXMit95* and *DXMit249*, and the lowest one locates to the interval between *DXMit89* and *DXMit50*. The LR test statistic scores thorough the X chromosome except the interval between *DXMit95* and *DXMit97* exceed 5 % critical value. The maximum LR score of 110.4 lies in the vicinity of *DXMit109*, and the estimated additive effect was 71.5. This QTL explains 46.7 % of the difference in the average net score of spermatozoal morphology between the X-B6/Y and X-MSM/Y males. The maximum LR scores in other two peaks were 51.3 at 1.8 cM and 79.7 at 57.0 cM, respectively, and the former explains 27.0 % and the latter explains 40.1 % of the difference. This result indicated that the difference of the net score between the X-B6/Y and X-MSM/Y is explained by these QTLs, and that at least three X-linked genes are involved in determining the trait.

3.3 A candidate gene responsible for the abnormal morphology of spermatozoa

In the interval between *DXMit50* and *DXMit147*, where the highest LR test statistic score is located, several genes that are expressed in the testis have been mapped. Fragile X mental retardation syndrome 1 homolog (*Fmr1*), androgen receptor (*AR*), SRY-box containing gene 3 (*Sox3*), haploid-specific alanin-rich acidic protein located on Chromosome-X (*Halap-X*) and DSS-AHC critical region on the X chromosome gene 1 (*Dax1*) were mapped in the region (Fig. 9). If they are candidates responsible for the morphological anomaly of the spermatozoa, the genes must be polymorphic between the C57BL/6J and MSM strains. I examined the polymorphisms of the

nucleotide sequences of these genes between the two mouse strains.

AR encodes a steroid hormone receptor consisting of 645 amino acids, which contains polyglutamine and polyglycine tracts in the transactivation domain. Comparison of the coding sequence of the C57BL/6J allele with that of the MSM allele revealed that there were polymorphic base substitutions at 5 positions, one of which results in amino acid substitution. Ile at the 527th position in the MSM allele was substituted by Leu in the C57BL/6J allele, both of which are hydrophobic residues. No polymorphic trinucleotide repeats were found in the transactivation domain. Because of GC-rich sequences in the Dax1 coding sequence, I failed to amplify the sequences in this study. Sequence analysis of *Fmr1* and *Sox3* is now underway.

The fifth candidate gene encodes haploid-specific alanin-rich acid protein on X chromosome (*Halap-X*). It was reported that the C57BL/6J allele of *Halap-X* encodes the protein with 239 amino acids, and that the protein is rich in basic amino acid in the region of the N-terminal one-third. In the same region, the nuclear localization signal exists. Two types of the acidic alanin-rich repeats are also found in the rest of the deduced protein (Taketo et al., 1997; Uchida et al., 2000). I looked for the polymorphisms in the nucleotide sequence of *Halap-X* between the C57BL/6J and MSM strain. I determined the sequence of the MSM allele and found that the protein has 298 amino acids deduced from the nucleotide sequence. The protein of the MSM allele contains two types of acidic repetitive sequences in the coding region: six-times repeat of the amino acid sequence, A-A-A-A-A-P-E-A-A-A-(S)-(P)-(E)-(S)-(S) (repeat a), and six-times repeat of the sequence, P-A-A-P-E-A (repeat b) (Fig. 10). Comparison

of the MSM and C57BL/6J alleles revealed that the C57BL/6J allele is 59 amino acids smaller than MSM allele, possibly due to a 162 bp deletion and an earlier termination codon in the C57BL/6J nucleotide sequence (Fig.10). The deletion reduced the number of the repeats of the two types of the acidic amino acid rich sequences in the C57BL/6J strain. To examine whether this polymorphism was observed in the genomic DNA or it reflects splicing variations of the mRNA, I analyzed PCR-amplified DNA sequence from genomic DNA of each strain as templates with the A8 primer pair set. The resultant sequences demonstrated that the PCR product from the genomic DNA of the C57BL/6J strain is smaller than that of MSM strain. Furthermore, the sequence of the cloned PCR products of the C57BL/6J cDNA was completely consistent to the data from the C57BL/6J genomic DNA. These results demonstrated that the C57BL/6J allele of *Halap-X* had 162-bp shortened genomic sequence.

4. Discussion

4.1 Candidate genes for the reduced testis weight

The highest LR statistic scores regarding the reduced testis weight are located to the distal region between *DXMit97* and *DXMit249* in the X chromosome. In this region, there are several candidate genes that are expressed in the testis. They are: extraembyonic, spermatogenesis, homeobox 1 (*Esx1*), phosphoribosyl pyrophosphate synthetase 1 (*Prps1*), procollagen, type IV, alpha 5 (*Col4a5*), ovary testis transcribed (*Ott*), Pyruvate dehydrogenase E1alspha subunit (*Pdha1*), and gap junction membrane channel protein alpha 6 (*Gja6*). One of them, *Esx1* encodes a transcription factor containing a homeobox domain, expression of which was detected in spermatogonia, proleptotene spermatocytes and round spermatids in the adult testis. The early transcription of *Esx1* in spermatogonia and proleptotene spermatocytes suggests that it functions in spermatogonial proliferation or spermatogenic meiosis. The late expression in round spermatids suggests its role in spermiogenesis (Banford et al., 1997). *Col4a5* encodes one of the major components of the basement membrane collagenous matrix and is expressed in seminiferous tubule basal laminae (Enders et al., 1995). *Ott* is expressed during meiosis in embryonic ovary and adult testis. *Gja6* is one of members of the connexin family of gap junction proteins and its expression is detected in the testis (Haeflinger et al., 1992). The functions of other candidate genes have not been defined yet. The further analysis of polymorphism in the candidate genes between C57BL/6J and MSM strains is needed to test whether the genes are

responsible for the phenotype.

Besides the candidate genes, there is the pseudoautosomal region (PAR) in the distal region of the mouse X chromosome. In the C57BL/6 strain, an X-linked gene *Mid1* straddles the boundary of PAR with three exons of the 5'-prime end located to the X-specific region and the remaining seven exons of the 3'-prime end located to the PAR (Perry et al., 2001). This gene was mapped between *DXMit249* and *DXMit160*. In another laboratory strain 129/SvEv, different exons of *Mid1* straddle the PAR. In *Mus spretus*, the whole exons of *Mid1* are located to X-specific region and are not included in the PAR. The sterility of (C57BL/6J × *M. spretus*)F1 males is most likely due to genetic diversity in the X-Y pairing region, leading to dissociation of the X-Y paring that is a prerequisite for spermatogenic survival through the meiotic process (Matsuda et al., 1982). These facts indicate that the distal region of mouse X chromosome has undergone rapid and substantial rearrangement during short period of time in speciation and subspeciation. The present QTL analysis mapped X-linked factor responsible for reduced testis weight to the distal region of the X chromosome, which may include PAR. The genetic divergence of the distal region of the X chromosome is likely to cause disruption or fragile X-Y pairing, and consequently spermatogenic breakdown.

Currently, I'm generating a congeneic strain that carry the critical distal region of the MSM-derived X chromosome beyond the marker *DXMit97* on the genetic background of the C57BL/6J strain. The preliminary study indicated that four out of 5 males of the congenic strain were fertile giving the average litter size of 8.0, and that

they had comparatively small testis of 69.5 mg. This indicates that the MSM-derived alleles in the distal region may not crucial for the sterility of the X-MSM/Y males.

4.2 Candidate genes responsible for the abnormal morphology of spermatozoa

The highest LR statistic score responsible for the spermatozoal anomaly is located to the central region between *DXMit50* and *DXMit95*, which contains the critical region at 29.0 cM mapped previously by Takagi (Takagi et al, 1994). In the interval, several genes that are expressed in the testis are mapped. They include fragile X mental retardation syndrome 1 homolog (*Fmr1*), androgen receptor (*AR*), SRY-box containing gene 3 (*Sox3*), haploid-specific alanin-rich acid protein located on Chromosome-X (*Halap-X*) and DSS-AHC critical region on the X chromosome, gene 1 (*Dax1*).

Fragile X syndrome is the most common cause of inherited mental retardation accompanied with macroorchidism in human (OMIM309550). *Fmr1* is transcribed ubiquitously, and its enhanced expression is observed in germ cells in both sexes, suggesting a function in gametogenesis. Human homologue of the mouse *Fmr1* is mapped to the X chromosome, Xq27.3 (The Dutch-Belgian Fragile X Consortium, 1994). *Sox3* is one of several Sox-genes and is expressed in urogenital ridge of mouse embryo, suggesting a function during testicular development. Human homologue of the mouse Sox3 is mapped on Xq26-q27 (Collignon et al., 1996). *Halap-X* is expressed in spermatid during spermiogenesis stage, suggesting a function for the chromosomal remodeling in spermatid nuclei. *DAX1* encodes a transcription factor that has been implicated in female sex determination and gonadal differentiation. The expression of

Dax1 is observed in several organs including adrenal gland, ovary and testis in adult mouse. Knockout mouse with null mutation for *Dax1* exhibited reduced testes weight, dysfunction of spermatogenesis and Leydig cell hyperplasia. It suggested *Dax1* has a function of the maintenance of spermatogenesis. Human homologue of mouse *Dax1* is mapped on Xq21.3 (Yu et al., 1998). The *AR* is essential for male sexual development and spermatogenesis, and they are extremely dependant on androgens. In human, trinucleotide repeat expansion in the *AR* gene causes reduced sperm production, testicular atrophy and infertility. Male mice carrying the *Ar* mutation show testicular feminization. Human homologue of mouse *Ar* is mapped on Xq11.2-q12 (Faber et al., 1991).

If MSM alleles of the above genes are not able to function in the C57BL/6J genetic background, defects of spermatogenesis or spermiogenesis might occurred. Thus, it is important to analyze the polymorphism of these candidate genes between the C57B L/6J and MSM strains.

4.3 Polymorphism of candidate genes between the C57BL/6J and MSM strains

I analyzed the polymorphism of nucleotide sequence of the candidate genes, responsible for the morphological anomaly of spermatozoa, between the C57BL/6J and MSM strains. I focused on one of candidate genes, haploid-specific alanin-rich acid protein located on Chromosome-X (*Halap-X*), because its presumed function in spermatogenesis meets the condition expected as candidate gene. Previous studies demonstrated that the Halap-X protein is predominantly present in the nucleoplasm of

round spermatids but gradually decreased as spermatids matured, followed by the subsequent appearance in the cytoplasm of elongating spermatids (Taketo et al., 1997; Uchida et al., 2000). Thus, the Halap-X prtotein is transferred from the nuclei to the cytoplasm during the spermatid maturation when the chromatin remodeling and chromatin condensation occur. The Halap-X protein may function in condensation of sperm chromatin. Most likely, acidic protein Halap-X facilitates specific association of nuclear DNA with some basic chromosomal proteins, and plays an important role in the process of chromatin condensation (Taketo et al., 1997; Uchida et al., 2000). Mutant mice bearing abnormal chromatin remodeling were known to produce morphologically abnormal and immotile spermatozoa (Cho et al., 2001; Yu et al., 2000). The morphology of the X-MSM/Y spermatozoa is characterized by the malformation of the sperm nuclei, which may be due to abnormal chromatin condensation. Therefore, it is possible that the candidate gene responsible for the spermatozoa morphology plays some functions in chromatin remodeling and condensation.

The sequencing of the MSM allele of *Halap-X* and comparison of the sequence with that of the C57BL/6J allele demonstrated that C57BL/6J allele has a deletion of 162 bp including the two types of the repeats of the acidic amino acid sequence and an earlier termination codon. One interpretation for the abnormal morphology of the X-MSM/Y spermatozoa is that the "longer-type" MSM allele of *Halap-X* cannot coordinate with the C57BL/6J allele(s) of autosomal and/or Y chromosomal gene(s), which results in improper chromatin remodeling, and

consequently produces abnormal spermatozoa. If this is correct, it would be possible to rescue the X-MSM/Y phenotype by transgenesis of the C57BL/6J allele of the *Halap-X* gene.

CHAPTER V General discussion

In very early stage of the reproductive isolation, F1 hybrids of the two diverging populations are viable and both sexes are fully fertile, but the progeny of F1 and the later generations show reduced fertility. Such reproductive isolation is sometime referred to as "hybrid breakdown" or "F2 hybrid breakdown". Study on the genetic basis of the hybrid breakdown provides profound understanding of the initiation stage of speciation process.

In order to investigate the early stage of the reproductive isolation, I employed genetic analysis of the sterility observed in males that carried the MSM strain-derived X-chromosome on the genetic background of the standard laboratory strains C57BL/6J on the way to establish a consomic strain B6.MSM-ChrX. Now, it is well known that the two mouse strains have originated from different subspecies, *M. m. molossinus* and *M. m. domesticus*. They have diverged from the common ancestor approximately one million years ago. The F1 and F2 hybrids between these two subspecies are viable, and both sexes are fully fertile. However, nobody has succeeded to establish inbred strains by continuous sib-mating beyond 20 generations from the F1 hybrids. In many cases, the litter size had been significantly reduced after the F5 to F7 generations and the both males and females of the mice became sterile (personal communications, K. Kondo, K. Moriwaki and T. Shiroishi). This clearly indicates that the two mouse populations are genetically discontinuous. In fact, recent phylogenic analysis based on the polymorphisms of the more than 1,700 microsatellite marker loci directly

demonstrated a significant genetic distance between the C57BL/6J and MSM strains (Kikkawa et al., 2001). Thus, the male sterility observed in the present study likely reflects the reproductive isolation in very early stage of speciation process.

Though many genes that are involved in hybrid sterility have been mapped so far, the studies on hybrid breakdown have been delayed. No gene responsible for the hybrid breakdown has been mapped in mouse. Because not a single gene but interaction between multiple genes is concerned in hybrid breakdown, the genetic system is more complicated and it has hampered the study on the hybrid breakdown. In this study, at least genes on X chromosome appeared to play essential roles in the initiation process of the reproductive isolation. This achievement would provide an indispensable clue to understand the whole genetic system of this reproductive isolation. In particular, it has made possible to explore autosomal or Y chromosomal gene(s) that interact with the X-linked genes.

From the result of the QTL analysis in this study, the reduced testis weight is caused by gene(s) on the distal region or chromosomal structure of the pseudoautosomal region on the X chromosome. Since histological anomaly of the testis is well correlated with the reduced testis size, it is possible that histological phenotype is also controlled by the same QTL. The reduced testis size and the histological anomaly may not be crucial for the sterility of the X-MSM/Y males, because proliferating spermatogenic cells and matured spermatozoa were observed in the X-MSM/Y males. Moreover, preliminary study on males of a congenic strain that carrying the critical distal region of the MSM-derived X chromosome on the C57BL/6J

genetic background showed substantial fecundity.

The sterility of the X-MSM/Y males is most likely attributable to the morphological anomaly and the reduced motility of the spermatozoa. Because of the reduced motility, the spermatozoa may fail to swim up to eggs in the oviducts *via* female reproductive tracts. In addition, the abnormal shapes of the sperm heads may make it difficult to penetrate sperms into the eggs *via* zona pellucida and cell membrane. The QTL analysis for the morphological anomaly of the spermatozoa successfully detected three distinct loci on X chromosome. The highest LR score is located to the central region of the X chromosome, where several candidate genes that are expressed in testis are mapped. Sequencing analysis in this study revealed that, one of candidate genes, *Halap-X*, has polymorphism in the large region of the coding sequences. The "long type" MSM allele may not function interactively with the C57BL/6J allele(s) of gene(s) in autosomes and/or Y chromosome. This incoordination may result in dysfunction of the chromatin remodeling and subsequent deformation of sperm nuclei.

In conclusion, the X chromosomal consomic strain, in which X chromosome is substituted between the two subspecies of *Mus musculus*, can be a useful model for the study of the initiation process of speciation. Moreover, it would shed light on understanding the genetic pathways of male reproduction system. Future analyses by mating experiments of the X-MSM/Y or B6.MSM-ChrX with the consomic strains for other autosomes would give answer which chromosome(s) is interactive with the X chromosome, and provide the full picture of the genetic pathway of the relevant

reproductive system

ACKNOWLEGEMENTS

I wish to express my sincere gratitude to my supervisor, Dr. Toshihiko Shiroishi, for his continuous advice, stimulating discussion and encouragement during all the stages of this work. I am grateful to Drs. Nobuo Takagi, Kiyotaka Toshimori and Toshiyuki Takano for their collaboration and discussion. I also thank Mr. Youichi Mizushina, Misses Noriko Sakurai and Hiromi Yamamoto for supporting and giving instructions of manipulating embryos and helpful suggestions. I greatly appreciate Mr. Akihiko Mita, Mrs. Toshie Aoki, Keiko Hiratsuka, Michiko Arii and other stuffs of animal facility of the National Institute of Genetics for supporting construction of the consomic strains and taking care of the mice used in this study. I also thank Drs. Tsuyoshi Koide, Masaru Tamura, Kunihiko Shimizu and other members of Mammalian Genetics Laboratory for valuable suggestions and support for this work.

REFERENCES

Branford, W. W., Zhao, G. Q., Valerius, M. T., Weinstein, M., Birkenmeier, E. H., Rowe, L. B. and Potter, S. S. (1997). Spx1, a novel X-linked homeobox gene expressed during spermatogenesis. Mech. Dev. 65, 87-98

Bartoov, B., Mayevsky, A., Sneider, M., Yogev, L. and Lightman, A. (1991) Sperm motility index: a new parameter for human sperm evaluation. Fertil. Steril. 56, 108-112

Basten, C. J., Weir, B. S. and Zeng, Z-B. (1996). *QTL Cartographer: a reference manual and tutorial for QTL mapping.* Department of statistics, North Carolina State University, Raleigh, NC.

Bonhomme, F. and Guenet, J-L. (1996). The laboratory mouse and its wild relatives. In *Genetic variations and strains of the laboratory mouse,* Lyon, M. F., Rastan, S., Brown, S. D. M . eds. Oxford University Press, pp 1577-1596

Cho, C., Willis, W. D., Goulding, E. H., Jung-Ha, H., Choi, Y-C., Hecht, N. B. and Eddy, E. M. (2001). Haploinsufficiency of protaminee-1 or –2 causes infertility in mice. Nature Genet. 28, 82-86

Collignon, J., Sockanathan, S., Hacker, A., Cohen-Tannoudji, M., Norris, D., Rastan, S., Stevanovic, M., Goodfellow, P. N. and Lovell-Badge, R. (1996) A comparison of the properties of Sox-3 with Sry and two related genes, Sox-1 and Sox-2. Development 122, 509-520

The Dutch-Belgian Fragile X consortium. (1994). *Fmr1* knockout mice: a model to study fragile X mental retardation. Cell 78, 23-33

Didion, B. A., Dobrinsky, J. R., Giles, J. R. and Graves, C. N. (1989). Staining procedure to detect viability and the true acrosome reaction in apermatozoa of various species. Gamete Res. 22, 51-57

Eicher, E. M., Washburn, L. L., Whitney, J. B., IV. and Morrow, K. E. (1982). *Mus poschiavinus* Y chromsome in C57BL/6J murine genome causes sex reversal. Science 217, 535-537

Eicher, E. M., Washburn, L. L., Shork, N. J., Lee, B. K., Shown, E. P., Xu, X., Dredge, R. D., Pringle, M. J. and Page, D. C. (1996). Sex-determining genes on mouse autosomes identified by linkage analysis of C57BL/6J-Y^{POS} sex reversal. Nature Genet. 14, 206-209

Eisner, J. R., Eales, B. A. and Biddle, F. G. (1996). Segeregating analysis of the testis-determining autosomal trait, *Tda*, that differs between the C57BL/6J and DBA/2J mouse strains suggests a multigenic threshold model. Genome 39, 322-335

Elliott, R. W., Miller, D. R., Pearsall, R. S., Hohman, C., Zhang, Y., Poslinski, D., Tabaczynski, D. A. and Chapman, V. M. (2001). Genetic analysis of testis weight and fertility in an interspecies hybrid congenic strain for Chromosome X. Mamm. Genome 12, 45-51

Enders G. C., Kahsai, T. Z., Lian, G., Funabiki, K., Killen, P. D. and Hudson, B. G. (1995). Developmental changes in seminiferous tubule extracellular matrix components of the mouse testis: alpha 3(IV) collagen chain expressed at the initiation of spermatogenesis. Biol. Reprod. 53, 1489-1499

Faber, P. W., King, A., van Rooij, H. C., Brinkmann, A.O., de Both, N. J, and Trapman, J. (1991) The mouse androgen receptor. Functional analysis of the protein and characterization of the gene. Biochem. J. 278, 269-278

Forejt, J. and Ivanyi, P. (1975). Genetic studies on male sterility of hybrids between laboratory and wild mouse (*Mus musculus* L.) Genet. Res. Camb. 24, 189-206

Forejt, J., Vincek, V., Klein, J., Lehrach, H. and Loudove-Michova, M. (1991). Genetic mapping of the *t*-complex region on mouse chromosome 17 including the Hybrid sterility-1 gene. Mamm. Genome 1, 84-91

Guenet, J-L., Nagamine, C., Simon-Chazottes, D., Montagutelli, X. and Bonhomme, F. (1990). *Hst-3* : an X-linked hybrid sterility gene. Genet. Res. Camb. 56, 163-165

Haefliger, J. A., Bruzzone, R., Jenkins, N. A., Gilbert, D. J., Copeland, N. G. and Paul, D. L. (1992). Four novel members of the connexin family of gap junction proteins. Molecular cloning, expression, and chromosome mapping. J. Biol. Chem. 267, 2057-2064

Haldane, J. B. S. (1992). Sex ratio and unisexual sterility in hybrid animals. J. Genet. 12, 101-109

Kikkawa, Y., Miura, I., Takahama, S., Wakana, S., Yamazaki, Y., Moriwaki, K., Shiroishi, T. and Yonekawa, H. (2001). Microsatellite database for MSM/Ms and JF1/Ms, molossinus-derived inbred strains. Mamm. Genet. 12, 750-752

Lee, K., Haugen, H. S., Clegg, C. H. and Braun, R. E. (1995). Premature translation of protaminee 1 mRNA causes precocious nuclear condensation and arrests spermatid differentiation in mice. Proc. Natl. Acad. Sci. USA 92, 12451-12455

Manly, K. F. and Olson, J. M. (1999). Overview of QTL mapping software and introduction to Map Manager QT. Mamm. Genome 10, 327-334

Matsuda, Y., Imai, H. T., Moriwaki, K., Kondo, K. and Bhnhomme, F. (1982). X-Y chromosome dissociation in wild derived *M. musculus* subspecies, laboratory mice, and their F1 hybrids. Cytogenet. Cell Genet. 34, 241-252

Matsuda, Y., Hirobe, T. and Chapman, V.M. (1991). Genetic basis of X-Y chromosome dissociation and male sterility in interspecific hybrids. Proc. Natl. Acad. Sci. USA. 88, 4850-4854

Perry, J., Palmer, S., Gabriel, A. and Ashworth, A. (2001). A short pseudoautosomal region in laboratpry mice, Genome Res., 11, 1826-1832

Pilder, S. H., Hammer, M. F. and Silver, L. M. (1991). A novel mouse Chromosome 17 hybrid sterility locus: implications for the origin of *t* haplotypes. Genetics 129, 237-246

Pilder, S. H., Olds-Clarke, P., Philips, D. M. and Silver, L. M. (1993). Hybrid sterility-6: A mouse *t* complex locus controlling sperm flagellar assembly and movement. Dev. Biol. 159, 631-642

Pilder, S. H. (1997a). Identification and linkage mapping of *Hst7*, a new M. spretus/M. m. domesticus Chromosome 17 hybrid sterility locus. Mamm. Genome 8, 290-303

Pilder, S. H., Olds-Clarke, P., Orth, J. M., Jester, W. F. and Dugan, L. (1997b). Hst7: A male sterility mutation perturbing sperm motility, flagellar assembly, and mitochondrial sheath differentiation. J. Androl. 18, 663-671

Takagi, N., Tada, M., Shoji, M. and Moriwaki, K. (1994). An X-linked gene governing sperm morphology revealed in laboratory mice consomic for X chromosome from Japanese house mouse, *M. musculus molossinus*. In *Genetics in wild mice*, Moriwaki et al. eds., Japan Sci. Soc. Press, Tokyo/S. Karger, Basel, pp 247-256

Taketo, M. M., Araki, Y., Matsunaga, A., Yokoi, A., Tsuchida, J., Nishina, Y., Nozaki, M., Tanaka, H., Koga, M., Uchida, K., Matsumiya, K., Okuyada, A., Rochelle, J. M., Nishimune, Y., Matsui, M. and Seldin, M. F. (1997). Mapping of eight testis-specific genes to mouse chromosomes. Genomics 46, 138-142

Toshimori, K. and Oura, C. (1993). Fine structural changes in the postacrosomal region of the hamster and mouse sperm head at the initial stages of gamete interaction. Arch. Histol. Cytol. 56, 109-116.

Toyoda, Y., Yokoyama, M. and Hoshi, T. (1971). Studies on the fertilization of mouse eggs in vitro. Jpn. J. Anim. Reprod. 16, 147-157

Trachtulec, Z., Mnulova-Fajdelova, M., Hamvas, R. M. J., Gregorova, S., Mayer, W. E., Lehrach, H. R., Vincek, V., Forejt, J. and Klein, J. (1997). Isolation of candidate hybrid sterility 1 genes by cDNA selection in a 1.1 megabase pair region on mouse chromosome 17. Mamm. Genome 8, 312-316

Uchisa, K., Tsuchida, J., Tanaka, H., Koga, M., Nishina, Y., Nozaki, M., Yoshinaga, K., Toshimori, K., Matsumiya, K., Okuyama, A. and Nishimune, Y. (2000). Cloning and characterization of a complementary deoxyribonucleic acid encoding haploid-specific alanin-rich acidic protein located on chromosome-X. Biol. Reprod. 63, 993-999

Whittingham, D. G., Leibo, S. P. and Mazur, P. (1972). Survival of mouse embryos frozen to -109° and -269°C. Science 178, 411-414

Wu, J. Y., Ribar, T. J., Cummings, D. E., Burton K. A., McKnight, G. S. and Means, A. R. (2001). Spermiogenesis and exchange of basic nuclear proteins are impaired in male germ cells lacking Camk4. Nature Genet. 25, 448 - 452

Yu, R. N., Ito, M., Saunders, T. L., Camper, S. A. and Jameson, J. L.,(1998). Role of Ahch in gonadal development and gametogenesis. Nature Genet. 20, 353-357

Yu, Y. E., Zhang, Y., Unni, E., Shirley, C. R., Deng, J. M., Russel, L. D., Weil, M. M., Behringer, R. R. and Meistrich, M. L. (2000). Abnormal spermatogenesis and reduced fertility in transition nuclear protein 1-deficient mice. Proc. Natl. Acad. Sci. USA. 97, 4683-4688

Zeng, Z-B. (1994). Precision mapping of quantitative trait loci. Genetics 136, 1457-1468

Fig. 1 Breeding scheme to generate X chromosomal consomic strain, B6.MSM-ChrX. (A) (C57BL/6J × MSM)F1 female was backcrossed to C57BL/6J male, and successive backcrosses to C57BL/6J males were repeated at least more than 10 generations. At each backcross generation, females with non-recombinant X chromosome from the MSM strain were selected, and used for cross of the next generations. Males with non-recombinant X chromosome of the MSM strain, X-MSM/Y, at different backcross generations were used in this study. (B) Twelve microsatellite markers located through X chromosome. Microsatellite markers except *DXMit166* and *DXMit193* were used for genotyping at each backcross generation. All markers were used in QTL analysis.

Fig. 1

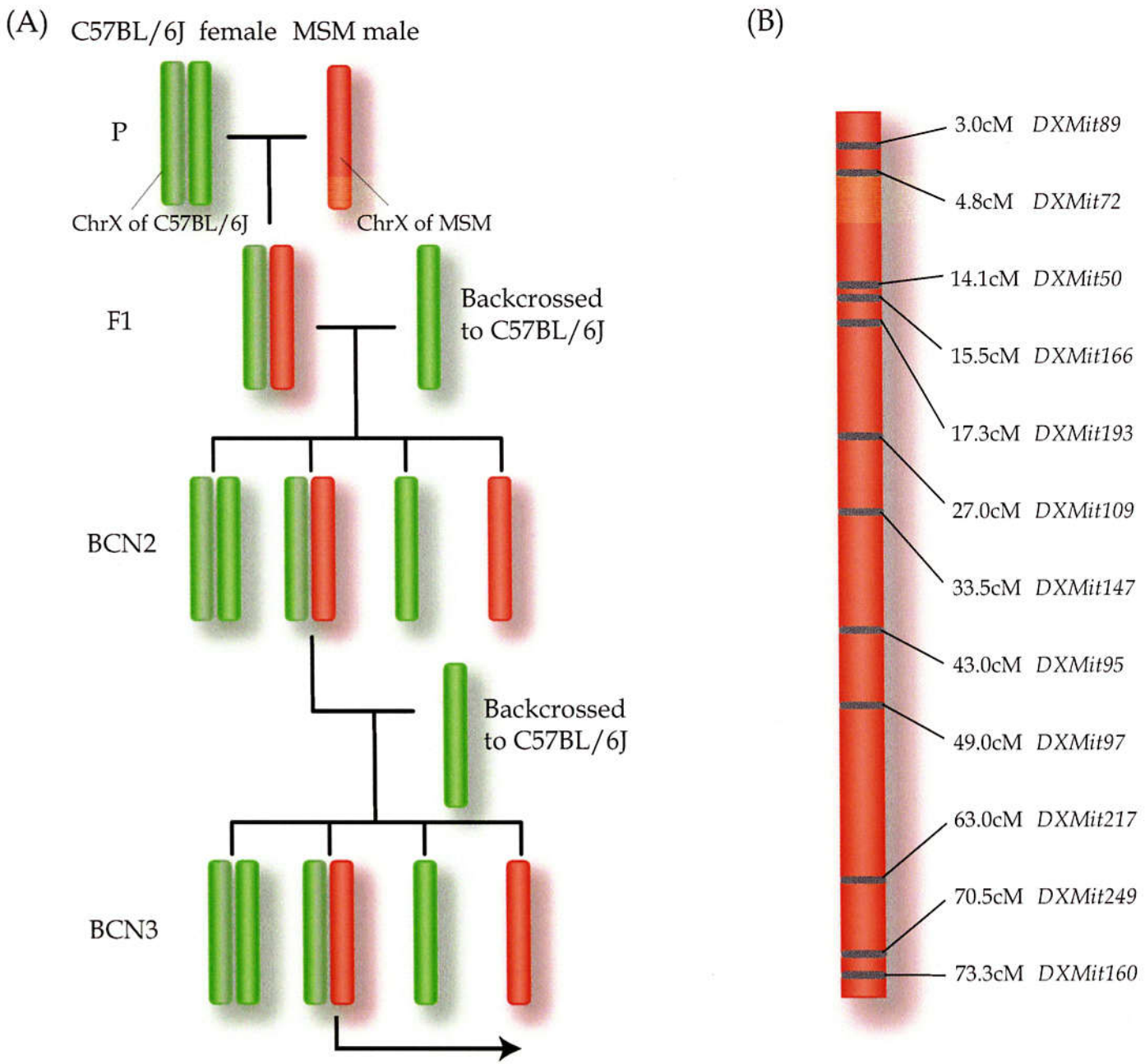
(A)
C57BL/6J female
MSM male
P
ChrX of C57BL/6J
ChrX of MSM
F1
Backcrossed to C57BL/6J
BCN2
Backcrossed to C57BL/6J
BCN3
(B)
3.0cM DXMit89
4.8cM DXMit72
14.1cM DXMit50
15.5cM DXMit166
17.3cM DXMit193
27.0cM DXMit109
33.5cM DXMit147
43.0cM DXMit95
49.0cM DXMit97
63.0cM DXMit217
70.5cM DXMit249
73.3cM DXMit160

Table 1. Reproduction of C57BL/6J, X-B6/Y and X-MSM/Y males in natural mating

	Backcross generation (No. of tested males)	No. of reproducible males	No. of females mated	No. of pregnant females	Mean Litter Size * per Fertile Pair
C57BL/6J	(9)	6	30	13	7.9 ± 1.9
X-B6/Y	BCN9 (4)	4	12	8	8.6 ± 1.1
X-MSM/Y**	BCN1 (10)	9	29	17	7.4 ± 1.3
	BCN2 (10)	9	30	21	5.0 ± 1.9
	BCN3 (10)	2	30	2	3.0 ± 0
	BCN9 (6)	0	18	0	0

*Values for mean litter size represent means ± SD.
**Values for mean litter size in X-MSM/Y males after BCN2 were significantly different from those in C57BL/6J males ($p < 0.05$).

Table 2. Fertilization analysis *in vivo* in X-B6/Y and X-MSM/Y males

	Sample*	No. of 1-cell-oocytes	No. of 2-cell-embryos	Fertilization	
				Rate (%)	Average rate (%)
X-B6/Y	1	3	10	76.9	80.4
	2	5	9	64.3	
	3	0	8	100.0	
	4	1	29	96.7	
	5	4	20	83.3	
	6	8	10	55.6	
	7	11	10	47.6	
	8	5	19	79.2	
	9	0	9	100.0	
X-MSM/Y	10	12	0*	0.0	0.0
	11	13	0	0.0	
	12	11	0	0.0	
	13	17	0	0.0	
	14	5	0	0.0	
	15	22	0	0.0	
	16	23	0	0.0	

*Individual number of X-B6/Y and X-MSMmales of BCN7 and BCN8 generation.

Table 3. Body and testicular weight of X-B6/Y and X-MSM/Y males (BCN5-7 generations)

	Body weight (g)*	Mean wight of paired testes(mg)*
X-B6/Y (n=16)	28.1 ± 2.9	94.4 ± 14.5
X-MSM/Y(n=12)	28.9 ± 2.6**	60.3 ± 12.0***

*Values for body and testis weight represent means ± SD.
**Significant difference was not ditected in body weight.
***X-MSM/Y males exhibited significantly smaller testes ($p < 0.01$).

Fig. 2 Histology of the testis of X-MSM/Y and X-B6/Y males at the BCN8 generation. The X-B6/Y testis (B) showed almost normal spermatogenesis as compared with the C57BL/6J testis (A), while the X-MSM/Y testis (C) showed thin and fragile epithelia with reduced number of spermatogenic cells. Another X-MSM/Y male showed severely degenerated seminiferous tubules that had lost most of the spermatogenic cells (*), and hyperplasia of Leydig cells (Ly) in the interstitial spaces adjacent to disrupted tubules (D). In the peripheral tubules, where spermatogenesis occurred, abnormal apoptotic germ cells were noted (arrow) (D). Differentiation of spermatogenic cells from the basal lamina to the lumen was observed in the C57BL/6J (E) and X-B6/Y testis (F), while the number of the differentiating spermatogenic cells was reduced in the X-MSM/Y testis (G). In the testis of the same X-MSM/Y male, severely degenerated tubules that contain only spermatogonia and Sertoli cells along the basal lamina were observed, and pachytene spermatocytes were sloughing into the lumen (arrows) (H). The cauda epididymal lumina of C57BL/6J male (I) were filled with mature spermatozoa, while the X-MSM/Y males showed many differentiating spermatogenic cells (arrow heads) as well as spermatozoa (J). Horizontal bar = 50 μ l

Fig. 2

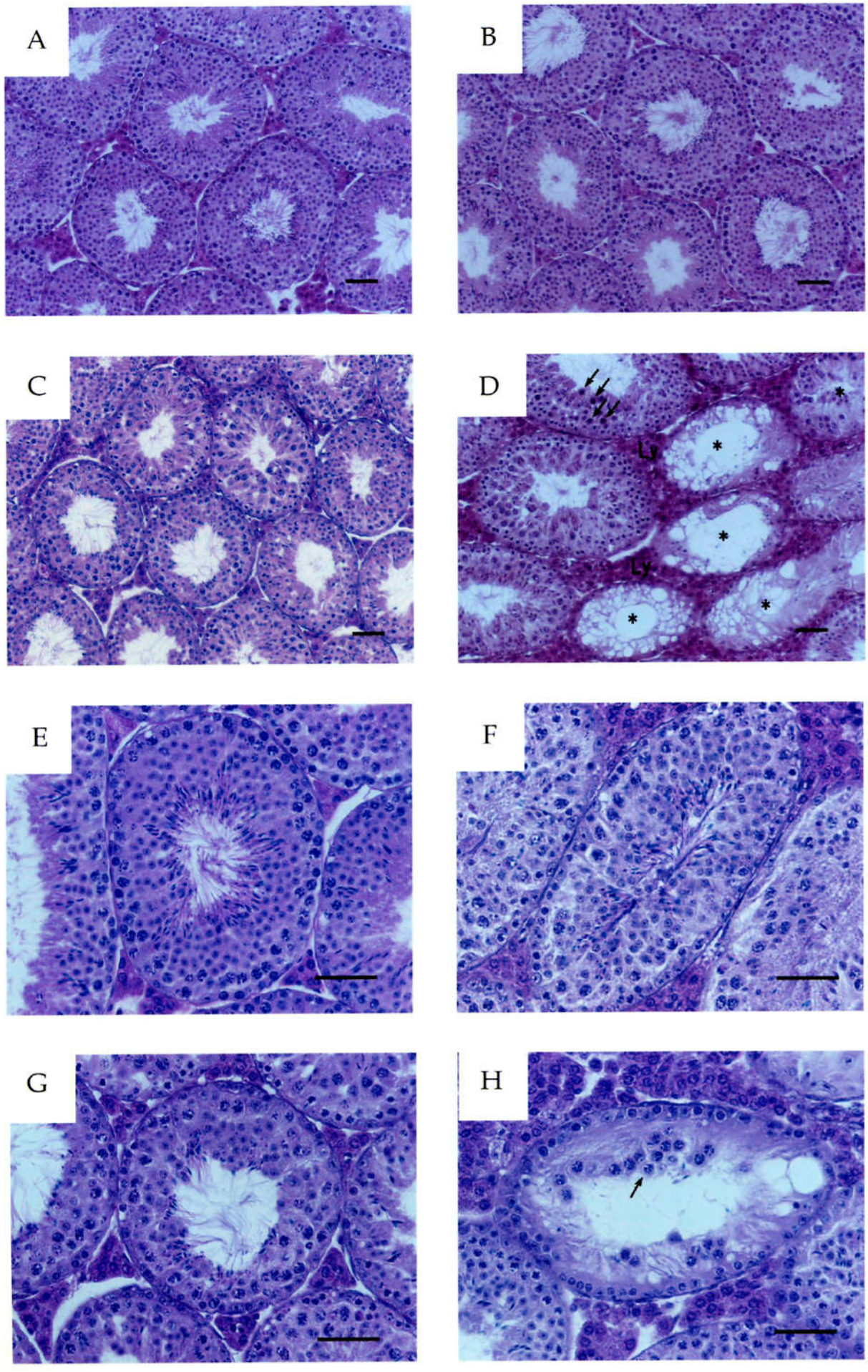

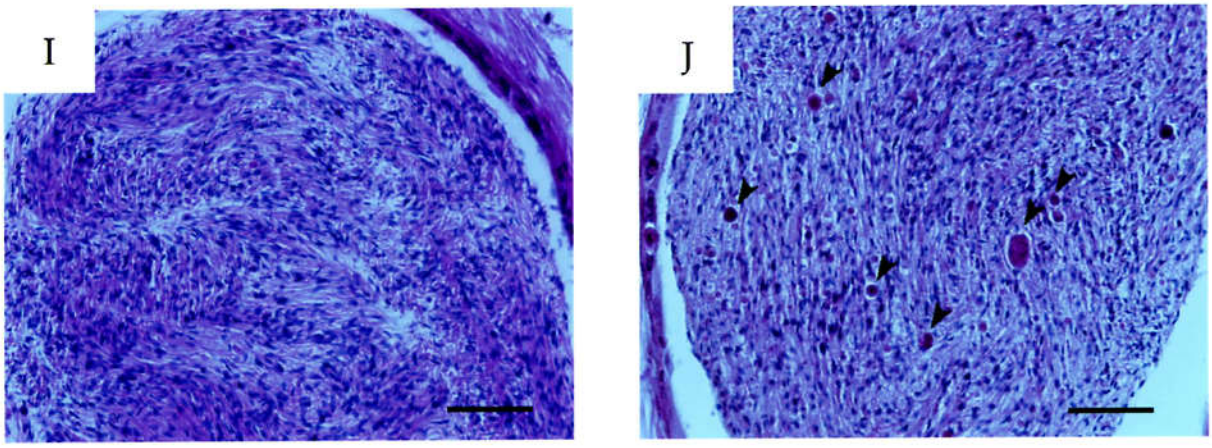
I
J

Fig. 3 Spermatozoa from X-B6/Y and X-MSM/Y males. C57BL/6J males had well-balanced and hook-shaped heads (A). Abnormal midpiece attachment sites (arrowhead) were occasionally observed in C57BL/6J males as well. X-B6/Y males at the BCN8 generation showed normal shape of sperm heads (B), while X-MSM/Y males showed slightly shortened distal region of the sperm heads (arrows) at the BCN2 generation (C). X-MSM/Y males at the BCN8 generation showed further shortened distal region (arrows) and squared postal region of sperm heads (arrow head) (D). Horizontal bar =100 μl

Fig. 3

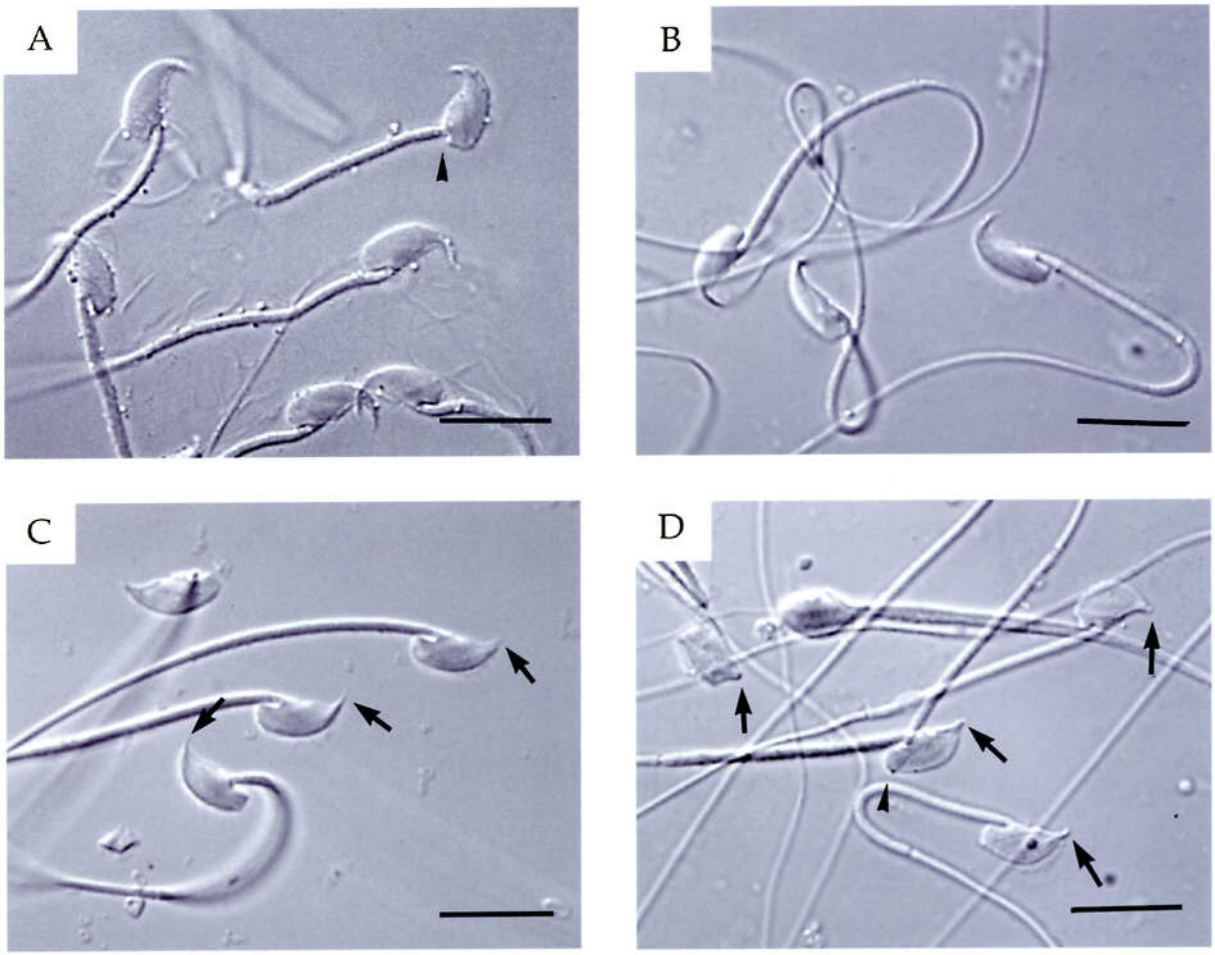

Fig. 4 Transmission electron micrographs of spermatozoa of X-B6/Y and X-MSM/Y males. Epididymal spermatozoa of the X-B6/Y males had regularly thin spindle-shaped sperm nuclei (A). X-MSM/Y males exhibited irregular shapes of nuclei. For example, an abnormal nucleus with two flagella profiles was observed (arrow) (B). High electron density of sperm nuclei was observed in both the X-B6/Y males (C) and the X-MSM-Y males (D), indicating the chromatin condensation. Acrosomes (ac) were observed even in the abnormal X-MSM/Y spermatozoa (D). The sperm nuclei of X-MSM/Y showed various types of deformed shapes (E, F). nu, sperm nuclei. Horizontal bar =1μl (A, B); Horizontal bar =0.5μl (C-F).

Fig. 4

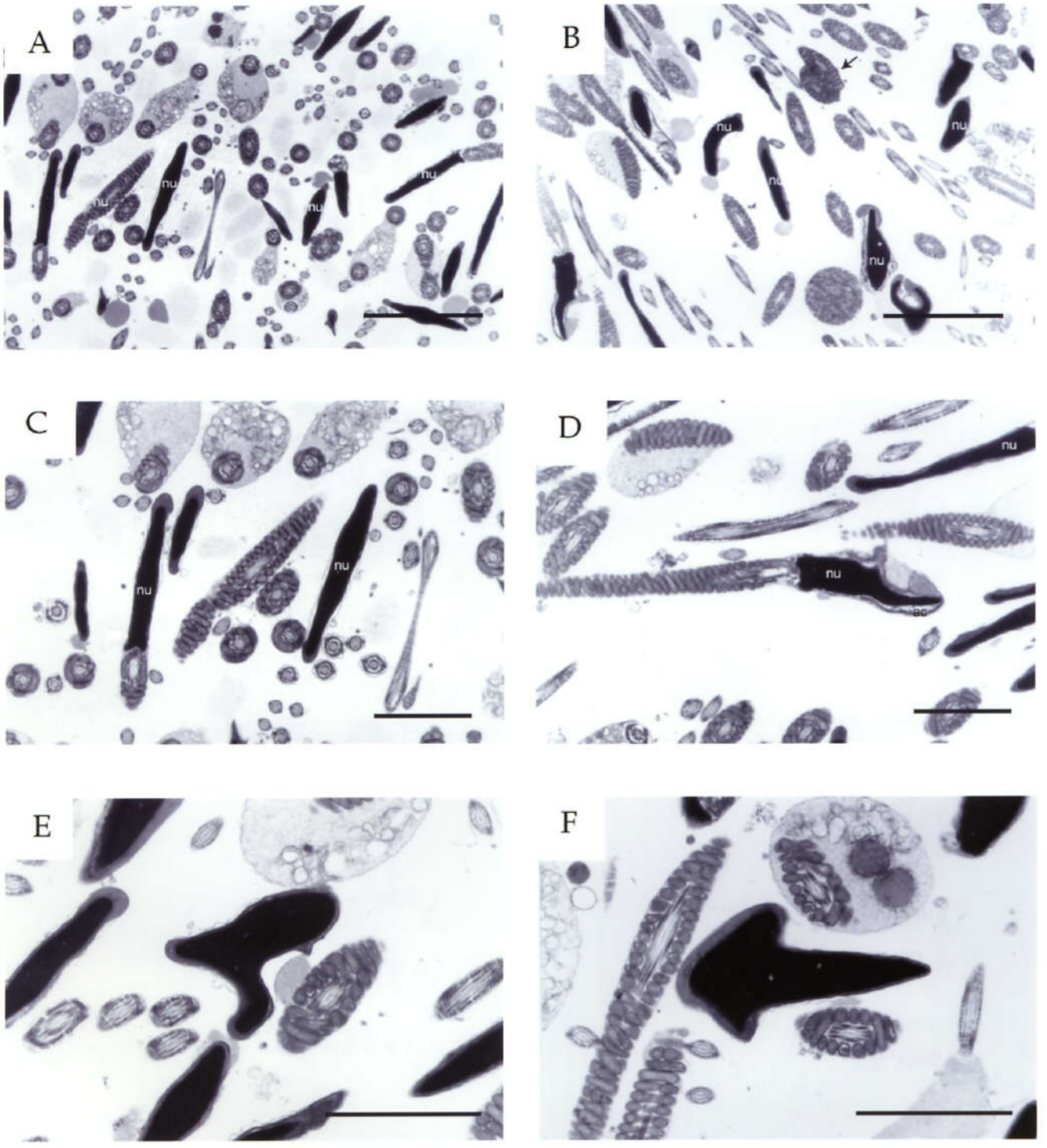

Fig. 5 Sperm motility index (SMI) of the spermatozoa of X-B6/Y and X-MSM/Y males at the BCN7 generation. The average SMI values (Mean ± SD, N = 5) of the X-B6/Y spermatozoa after 1, 2, 3 and 4 hrs of incubation time were 163.6 ± 28.6, 199.6 ± 36.1, 187.3 ± 47.2 and 152.8 ± 24.0, respectively (green solid line). The average SMI values (Mean ± SD, N = 5) of the X-MSM/Y spermatozoa at the same incubation times were 84.2 ± 17.5, 88.3 ± 20.4, 83.3 ± 21.5 and 72.8 ± 22.1, respectively (red solid line). The SMI values of the X-MSM/Y spermatozoa were significantly lower than those of the X-B6/Y spermatozoa through all the incubation times ($p < 0.001$).

Fig. 5

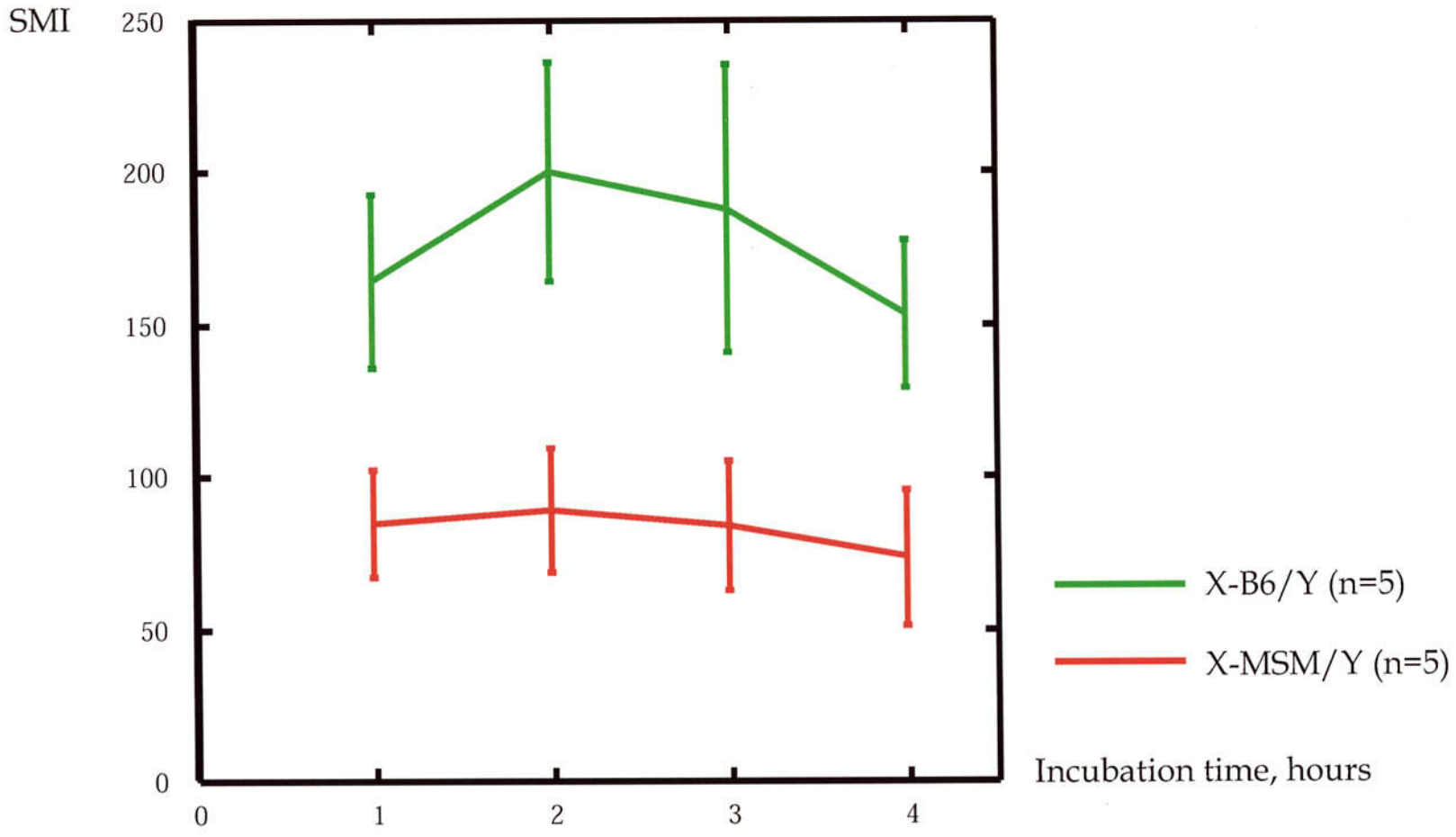
SMI
250
200
150
100
50
0
0
1
2
3
4
X-B6/Y (n=5)
X-MSM/Y (n=5)
Incubation time, hours

Fig. 6 Result of QTL analysis for the testis weight using the BCN5-7 backcross progeny generated from the heterozygous (X-MSM/X-B6) females. Likelihood ratio test statistic is plotted at every 1 cM interval. The 5% critical value is indicated by a dotted line.

Fig.6

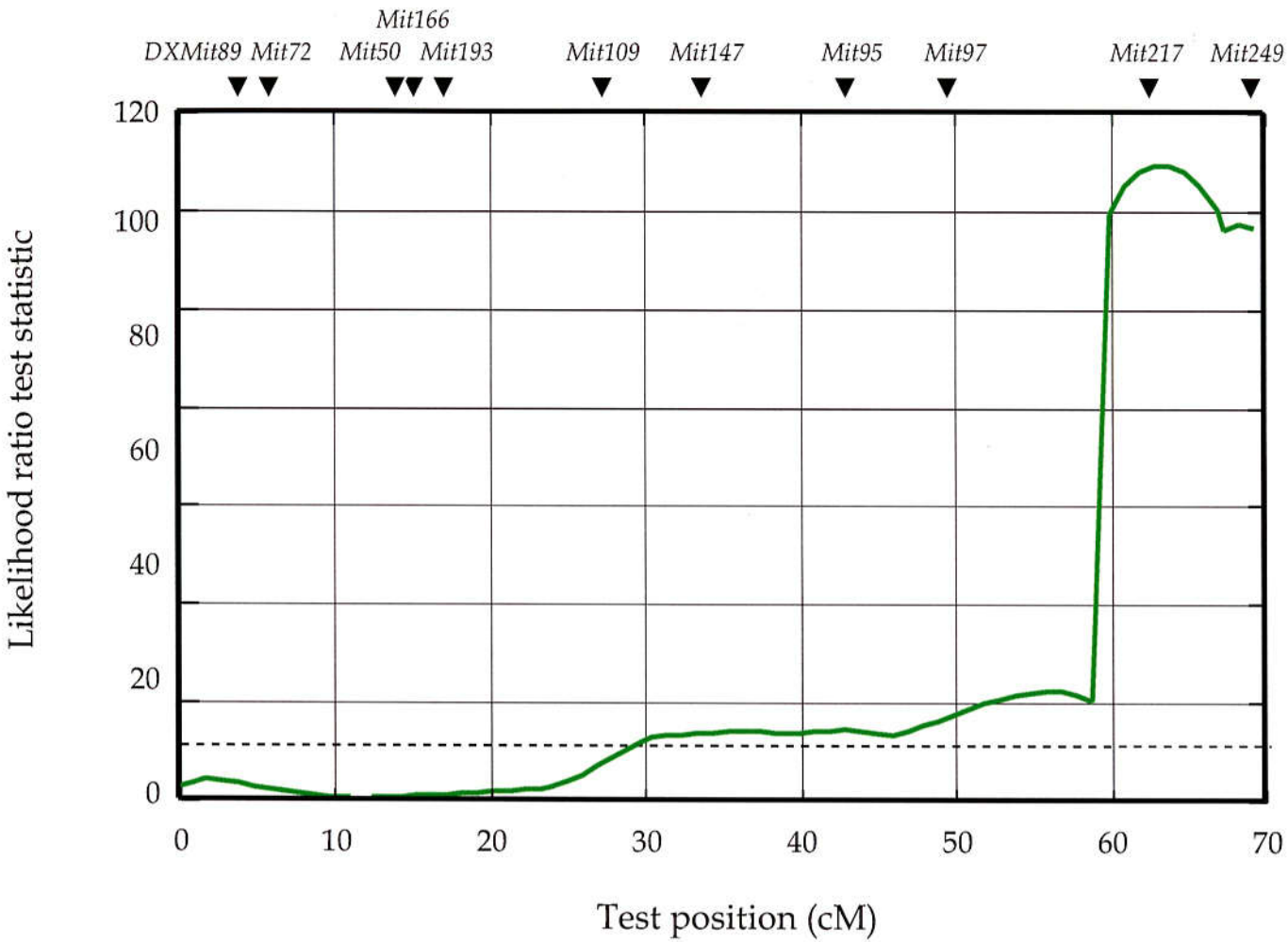
DXMit89
Mit72
Mit166
Mit50
Mit193
Mit109
Mit147
Mit95
Mit97
Mit217
Mit249
120
100
80
60
40
20
0
0
10
20
30
40
50
60
70
Likelihood ratio test statistic
Test position (cM)

Fig. 7 Quantification of morphological anomaly of sperm head. Sperm heads were classified into 6 types regarding the severity of morphological anomaly of spermatozoa (A). Type 1 is normal. The abnormality becomes severer in the order of type 2 to type 6. Majority of spermatozoa from X-MSM/Y males at the BCN5-7 generations were classified into type 4. The morphological anomaly of the spermatozoa was calculated for the QTL analysis (B). X-MSM/Y (BCN5-7) males, the permatozoal morphology of which was severely affected, gave a high score, 326.2, while X-B6/Y males gave a low score, 19.8 (B).

Fig. 7

(A)

	Type1	Type2	Type3	Type4	Type5	Type6
						
	Normal					Abnormal
Score	0	1	2	3	4	5
X-B6/Y n=19	**87.0%**	8.4%	3.1%	1.3%	0.2%	0.1%
B6.MSM-ChrX n=14	0%	4.0%	1.6%	**71.0%**	13.3%	10.6%

(B)

Calculation to evaluate spermatozoal morphology

Score of X-B6/Y

$(0\times87.0)+(1\times8.4)+(2\times3.1)+(3\times1.3)+(4\times0.2)+(5\times0.1)$ = **19.8**

Score of X-MSM/Y

$(0\times0)+(1\times4.0)+(2\times1.6)+(3\times71.0)+(4\times13.3)+(5\times10.6)$ = **326.2**

Fig. 8 Result of QTL analysis for the sperm anomaly using the BCN5-7 backcross progeny generated from the heterozygous (X-B6/X-MSM) females. Likelihood ratio test statistic is plotted at every 1 cM interval. The 5% critical value is indicated by a dotted line.

Fig. 8

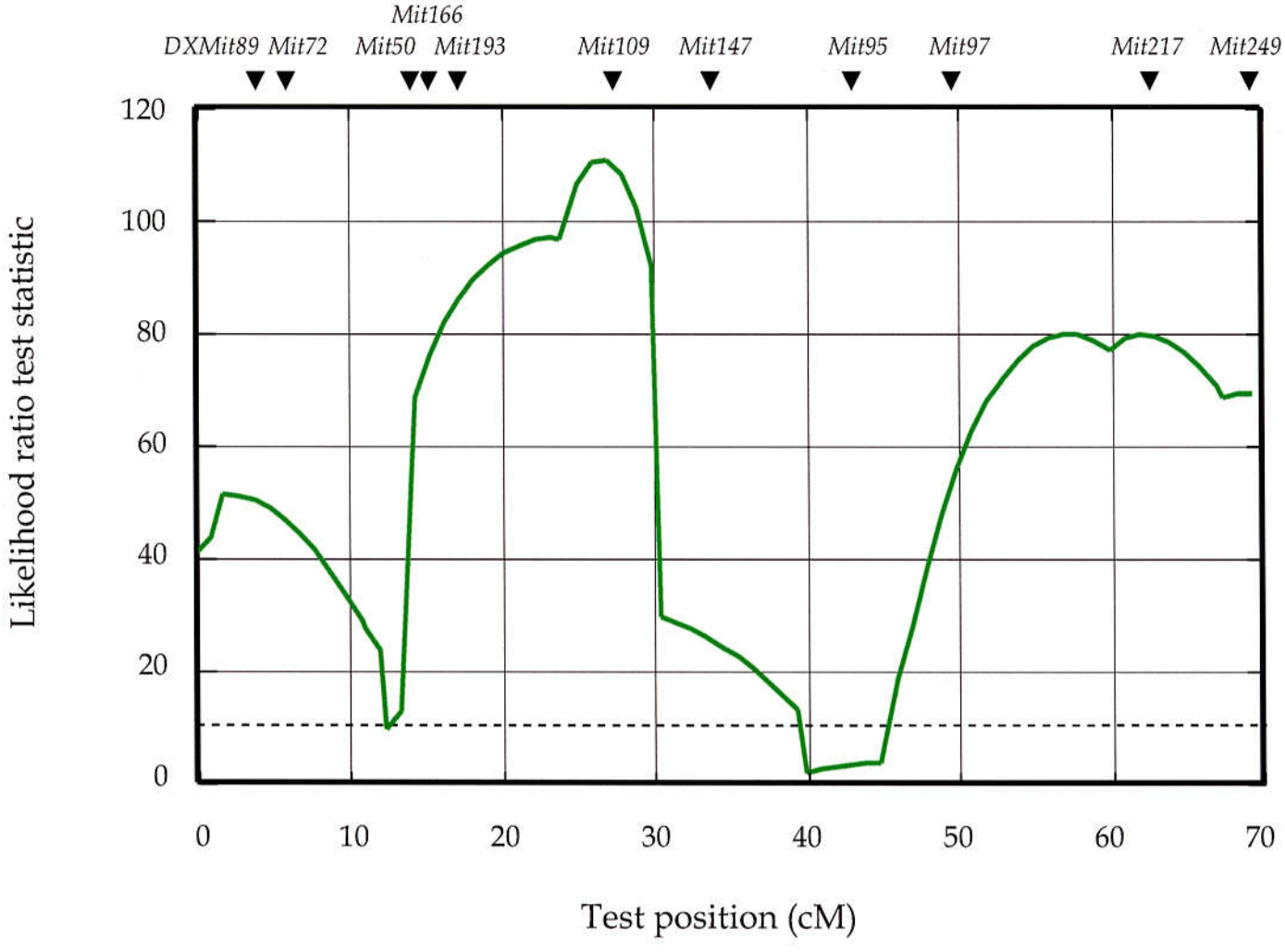
DXMit89
Mit72
Mit166
Mit50
Mit193
Mit109
Mit147
Mit95
Mit97
Mit217
Mit249
120
100
80
60
40
20
0
0
10
20
30
40
50
60
70
Likelihood ratio test statistic
Test position (cM)

Fig. 9 Candidates genes responsible for the quantitative traits of X-MSM/Y males. Six and five genes, which are candidates for the reduced testis weight and the morphological anomaly of spermatozoa respectively, are mapped to the regions in the vicinity of each QTL on the X chromosome. X-specific region-pesudoautosomal region boundary is located to the interval between *DXMit249* and *DXMit160*.

Fig. 9

Candidate genes for reduced testis weight and sperm anomaly

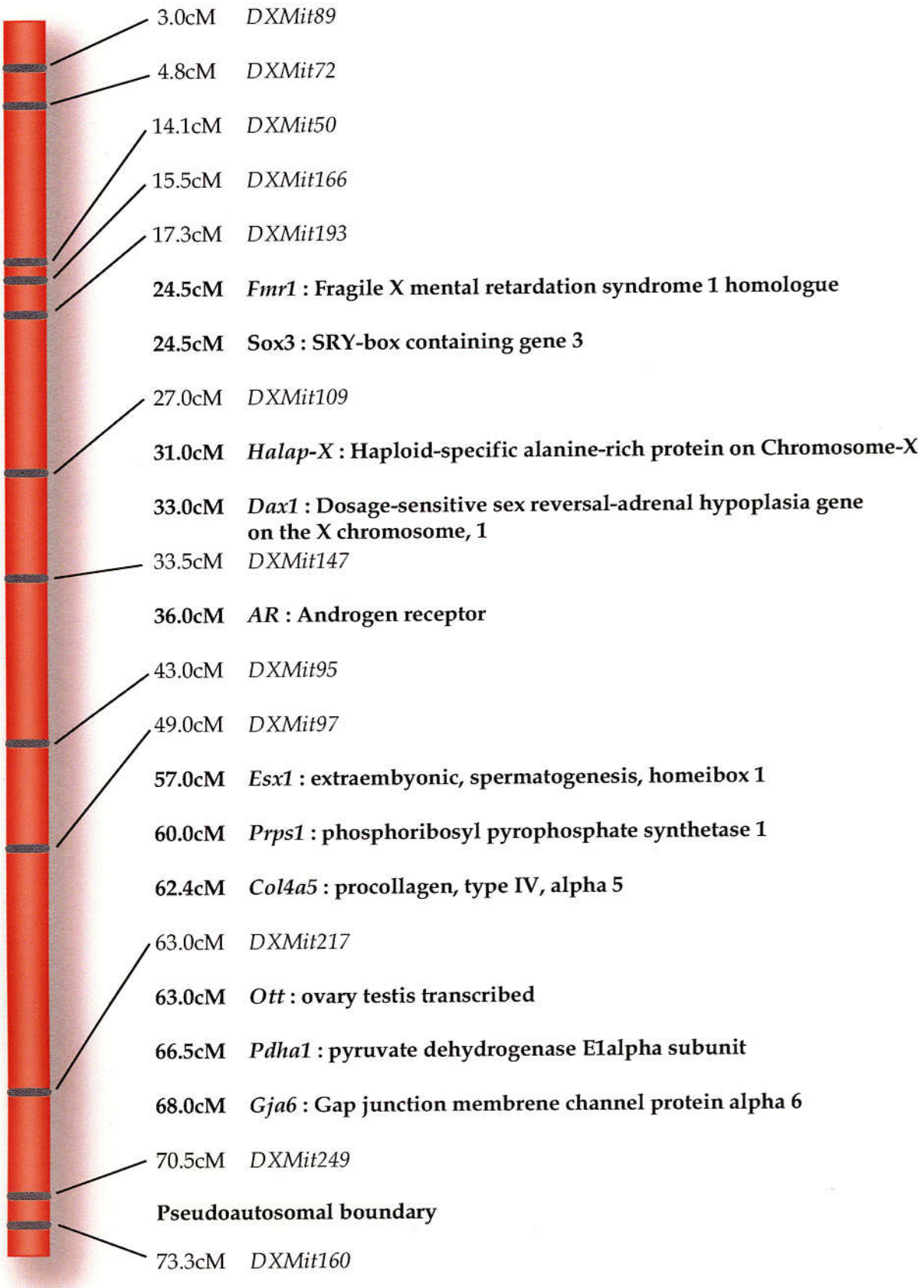

Fig. 10 Polymorphism of *Halap-X* between C57BL/6J and MSM strains. Amino acid sequences of these two strains are directly compared (A). Asterisks stand for identical amino acid residues between two strains, and green boxes indicate polymorphic regions. Pink and blue boxes depict acidic repetitive sequences, A-A-A-A-A-P-E-A-A-A-(S)-(P)-(E) -(S)-(S) (repeat a) and P-A-A-P-E-A (repeat b). The polymorphic regions between C57BL/6J and MSM are illustrated (B).

Fig. 10

(A)

```
MSM       MDVPTSSTDSQEVKPIMPIRTKAACKFYPPHILCGKGAKT
C57BL/6J  MDVPTSSTDSQEVKPIMPIRTKAACKFYPPHILCGKGAKT
          ****************************************

MSM       NKRGKRGGAQKASTKKDIGETTPPVAKKSKVAKEPTVLAA
C57BL/6J  NKRGKRGGAQKASTKKDIGETTPPVAKKSKVAKEPTMLAA
          ************************************ ***

MSM       AAAPEAAASPESSAAAAAPEAAASPESSAAAAAPEAAASP
C57BL/6J  AAAPEAAASPESSAAAAAPEAAASPESSAAAAAPEAAASP
          ****************************************

MSM       ESSAGAAAAPEAAASPESSAAAAAPEAAASLESSVAAAAP
C57BL/6J  ESSAGAAAAPEAAASLESSAAAAAPEAAA----------
          *************** **********

MSM       EAAASLESSAAEAAPEAPPAPEVAAAPATPAAPEAAAAPE
C57BL/6J  ----------------------------------------

MSM       VAAAPATPAAPEAAAAPEVAAAPATPAEPEATAAPAGPEA
C57BL/6J  ---APATPAAPEAAAAPEVAAAPATPAAPEATAAPAAPEA
             ************************ ************

MSM       ATTPAAPEAPAAAPAVEEEEMVWEAAAVVGEAAVKPPEEE
C57BL/6J  ATTPAAPEAPAAAPAVEEEEMVWEAAAVVGEAAVKPPEEE
          ****************************************

MSM       PTSGEAVATTTMTYADSQ
C57BL/6J  PTSGEAVATTTMT
          *************
```

(B)